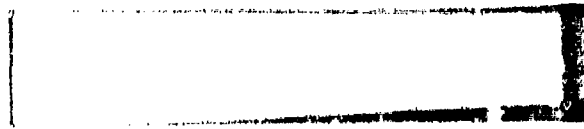


AD A119114

12



DTC FILE COPY

This document has been approved for public release and its distribution is unlimited.

DTC
SEP 08 1982

HYDRONAUTICS, incorporated research in hydrodynamics

Research, consulting, and advanced engineering in the fields of NAVAL and INDUSTRIAL HYDRODYNAMICS. Offices and Laboratory in the Washington, D. C., area: Pindoll School Road, Howard County, Laurel, Md.

82 09 08 022

HYDRONAUTICS, Incorporated

TECHNICAL REPORT
8268-1

SELF RESONATING PULSED WATER JETS
FOR AIRCRAFT COATING REMOVAL:
FEASIBILITY STUDY

by

Georges L. Chahine
Virgil E. Johnson, Jr.
and

Gary S. Frederick

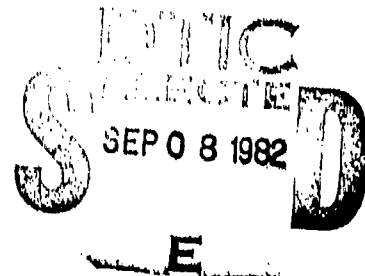
June 1982

The information in this report is based upon work supported by

The Department of Defense
Defense Small Business Advanced Technology Program
Office of Naval Research
Arlington, VA 22217

Under

Contract No: N00014-82-C-0143



This document has been approved
for public release and sale; its
distribution is unlimited.

HYDRONAUTICS, Incorporated

-ii-

FOREWORD

This report was prepared by HYDRONAUTICS, Incorporated, Laurel, Maryland under ONR Contract No. N00014-82-C-0143. The Scientific Officer for this contract was Mr. David Siegel, Code ONR 260. The authors wish to acknowledge the valuable discussions and suggestions provided by Mr. Siegel during this program.

We also want to thank Mr. Gary Gates, Code 61225, Naval Island Naval Air Station, for providing all of the test panels used during this effort, and for his important guidance in the real-life aspects of aircraft cleaning. The assistance and counsel provided by Dr. Andrew F. Conn and Mr. George E. Matusky, HYDRONAUTICS, is gratefully acknowledged.

PATENTS

The principles of passive jet excitation described in this report were included in U. S. Patent Application Serial Number 215,829, by V. E. Johnson, Jr., HYDRONAUTICS, Incorporated dated December 12, 1980, and subsequent U. S. continuations and Foreign Applications.

SUMMARY

This study examined an innovative technique to augment the efficiency of water jets and the degree of their control in removing aircraft coatings and preparing surfaces for recoating. It dealt specifically with a passive disruption of a waterjet into slugs in order to produce high-frequency, high-pressure shock wave impacts. The approach was to use self-resonating chambers, which amplified and structured the turbulent shear layer of the jet. The acoustical oscillations produced were tuned to the predominant natural frequencies of the nonexcited jet. The main objective of this phase of the research program, which was to establish if self-resonating nozzles are able to produce, at a relatively large standoff distance, a train of slugs capable of removing aircraft coating; at a high and controllable rate, was successfully achieved.

To meet this objective, two types of resonating nozzles were built and tested against various types of coatings defined after consultation with the U.S. Navy. The results were compared with a conventional nozzle. A more fundamental, parallel approach was followed in order to correlate the resonance characteristics with the impact forces imparted on the eroded surface.

The experimental study shows that the bunching characteristics of the jet correspond to the acoustical measurements of pressure oscillations in the nozzle tube. The frequency spectrum of these oscillations perfectly correlated with that of the pressure fluctuations on a transducer target. A new technique consisting of measuring the oscillations of the interrupted light of a laser beam onto a photo multiplier has also shown a perfect correlation with the preceding spectra. The oscillation frequencies as well as the bunching characteristics (wave length, optimum standoff distances) are correctly predicted with a preliminary analysis.

HYDRONAUTICS, Incorporated

-iv-

Paint cleaning tests were performed both on carbon-fiber reinforced composites and aluminum panels. The composite panel tests were not significant due to large discrepancies in the paint and material properties. Very positive results were obtained with the aluminum panels which showed great improvement relative to a standard jet at high standoff distances. We are confident that well optimized self-resonating pulsed jets can overcome the drawbacks of existing water jet methods, and provide a practical replacement or primary supplement for chemical removal methods.

I. INTRODUCTION

A. Objective

The objective of this project was to investigate the feasibility of disrupting a high pressure water jet into a discrete train of well organized slugs through passive acoustic self-excitation of the jet, and as a result to enhance the ability of the jet to remove aircraft coatings and to prepare surfaces for recoating. This innovative technique takes advantage of the water hammer pressures produced by the slugs' impact (which are much higher than the stagnation pressures generated by a continuous jet), without the drawbacks of having a mechanical rotating interrupter. In addition this technique provides larger working standoff distances, wider areas of impact and thus greater control of the energy imparted to a target than a cavitating jet. It is therefore capable of overcoming the drawbacks of existing water jet methods in preparing aircraft surfaces for repainting and of providing a primary supplement if not a practical replacement for chemical removal methods.

This first phase of the research concentrated mainly on a qualitative assessment of the self-oscillating jets (SERVOJETS), in the development of techniques able to rapidly quantify the bunching characteristics of subsequently designed SERVOJETS, and in a limited quantitative assessment of the cleaning power of this jet on aluminum and carbon-fiber reinforced aircraft panels. Another important objective was to determine the existence of a correlation between the geometrical appearance of a jet, its acoustical characteristics and the generated pressures on a target. Such a correlation allows one to concentrate on the geometrical and acoustical properties of the jet in any future optimization of the SERVOJET's nozzles.

B. Background

Coatings applied to aircraft surfaces for aesthetic reasons or for protection are periodically removed for repair and re-coating. Preparation of the surfaces and coating removal is presently accomplished mainly with chemicals.

The chemical stripping procedures now used are slow, costly, dangerous to personnel, and environmentally unsafe without substantial controls. Both the U.S. Navy and Air Force are actively seeking a replacement for chemical paint strippers and removers. Various types of mechanical techniques have been examined; water jets, carbon dioxide pellets, as well as various abrasive-grit blasts and lasers. All of these methods, however, have the same drawback -- namely, a strong potential for damaging the substrate. Laser blasting is promising, but requires revolutionary improvements in the state-of-the-art before becoming economically viable.[1].

Laboratory experiments involving the removal of paint from aluminum and glass fiber reinforced plastic (GFRP) substrates have demonstrated the basic selectivity of the water jet erosive process in comparison with the chemical procedures. While chemical stripping attacks indiscriminately both top coat and primer, we found in earlier tests performed at HYDRONAUTICS, Incorporated with cavitating jets that the lower "erosion strength" (i.e., energy needed to be removed from the panel), S, of the polyurethane-based top coat allowed it to be removed with little or no damage to the epoxy-based primer ([1], Table 2). The erosion strength of this primer was nearly the same as the aluminum panel, and substantially greater than that of the GFRP. Indeed, as we will underline later in this report, this concept of relative "erosion-strength" of various coatings and of the substrate is to be emphasized. For example, in situations where

the substrate erosion strength is less than or equal to that of the coating, no purely mechanical method can remove 100 percent of that coating without taking away some of the substrate. Fortunately, however, during standard aircraft overhauls, it is desirable not to remove an intact and well-bonded primer [2]. The "selectivity" of water jets which we have observed, as noted above, makes water jets more effective in this case than chemical strippers for most normal maintenance of Navy or Air Force equipment. The same reasoning suggests that worn top coats and primers for deteriorated coatings can be easily removed with no damage to the aircraft surfaces. For all such applications, self-resonating pulsed jets would be much more effective than regular jets, as higher impact forces would be imparted on a larger cleaning surface.

In a study supported by the Air Force [1], it was concluded that water jets showed the greatest promise among the several mechanical coating removal techniques which were considered. As discussed below, self-resonating pulsed jets have intrinsic advantages in comparison to any other type of water jet -- when attempting to remove coatings from the complex, and readily-damaged surface of an aircraft.

The potential advantages of an interrupted jet compared to a continuous one are quite well-known and have been of interest for jet erosion enhancement for a long time. While the pressure produced by a continuous jet on a target is of the same order of magnitude as the stagnation pressure, $\frac{1}{2} \rho V^2$ (where ρ is the liquid density and V is the jet speed), it is of order ρcV (where c is the speed of sound in the liquid) after each impact for a train of slugs. This basic interpretation shows that by producing discrete water packets one can take advantage of impact forces, an order of magnitude higher than in the continuous

case, to initiate and then propagate microcracks in the coating to be removed. In addition, the produced slugs have a greater ratio of impact area to water volume which enhances the surface cleaning effectiveness and introduces, through the standoff distance variable, an additional degree of control of the cleaning rate. More importantly, the cyclical unloading generated with a train of slugs produces absolute tensions which promote fractures and unbonding of the various coating layers from each other and from the substrate.

At this time, although an admittedly promising way to utilize water to cut and clean, pulsed jets are not operational, due to the lack of a practical, nonintrusive method for interrupting the jet. Devices using a rotating perforated disc have often been used, and results showing the efficiency of such devices have been reported, for instance, by Lichtarowicz, et al. [3], Summers [4], Erdmann-Jesnitzer, et al. [6], and Janakiram, et al. [6]. Discrete water packets have also been obtained by water cannons [7], achieving very high exit velocities. However, only very low repetition rates are possible, and the practicality of such devices is limited due to the high stresses developed within the nozzle. The most interesting mechanically interrupted or modulated jet is that developed by Nebeker [8]. It has the advantage of being self-contained and self-driven. However, being based on a mechanical interruption of the jet makes it present the disadvantages of rapid wear, probably due to cavitation erosion in the slots and to friction, and thus to a very short lifetime, and noncontrolled frequencies of the modulator.

Obtaining passively, without any moving parts, the modulation of the jet has the great advantage of achieving an appreciable increase of material removal efficiency, with minimum losses, no wear problems and no need for any additional external source

of power. In addition, it has the advantage of generating controlled frequencies which are not time dependent since the system is free of wear problems. As we will see below these frequencies are much higher than those used in mechanical devices and correspond to the desired optimum frequencies for maximum material removal efficiency of the jet. The possibility of extending, if desired, the effective range of the modulated jet (maximum standoff distance for optimum cutting rate) by air or water-sheathing adds to the relevance of this innovative technique.

II. SERVOJET CONCEPTS

A. Background

For over 10 years, HYDRONAUTICS, Incorporated has been engaged in the development of high-speed cavitating jets for numerous applications including drilling, mining, and cleaning. The CAVIJET® cavitating fluid jet method is one of the very few successful attempts to harness, for useful purposes, the destructive power of cavitation. One of the recent developments in our CAVIJET program is passive, self-resonating devices for modulating the flow in CAVIJET nozzles. These simple devices operate most effectively in the frequency range, f , corresponding to a Strouhal number ($S = fd/V$) between 0.3 and 1.2, and have produced rms amplitudes in some configurations as high as 50 percent of the mean jet flow (d is the jet diameter).

The principle of the basic CAVIJET, which consists of a submerged jet, is to produce cavitation in the shear zone between the jet and the surrounding liquid. The cavitation observed in this zone has the tendency to be moderately structured in ring vortices with a preferred period [9]. These rings become discrete and the jet very structured when the flow is excited at the preferred frequency which corresponds to a Strouhal number of approximately 0.3 [10,11]. This observation was already known for air-jets [12]; when excited very moderately for the same approximate Strouhal number, the flow becomes highly structured into a sequence of ring vortices persisting for several jet diameters downstream of the nozzle exit. Many investigators [12-16] have examined phenomena related to fluctuating jets, either self resonating or with an external means for stimulating or driving the pulsations in the jet flow. Schematics of several concepts available for pulsing jets are

shown in Figure 1. The basic principle of the search for a resonating jet is mainly to find a way of matching its predominant turbulent frequency with that of the resonator. For self-resonance the resonator has to be nonintrusive. An organ-pipe resonant chamber or a Helmholtz resonant oscillator (Figure 2) are among the several rather simple devices already tested successfully at HYDRONAUTICS for underwater cavitating jets.

The SERVOJETS studied in this project are the same types as those already tested in submerged conditions and can be grouped into three types. They have been given the descriptive names: "PULSER SERVOJET", "PULSER-FED SERVOJET" and "ORGAN-PIPE SERVOJET". The concept for each type will now be described.

B. PULSER SERVOJET

The configuration for this self-resonating jet concept, a tandem-orifice Helmholtz resonator, is shown in Figure 2a. The steady, high-pressure flow enters through the feed line, diameter, D_F , and passes through an entrance section of length, L_p , and diameter, D_p . The flow then contracts through the first orifice: d_1 , passes through the chamber (volume: V ; length, L ; diameter: d_T) and exits through the second orifice, d_2 .

If operated at its optimum Strouhal number, $S_d = fd_1/V_1$, discrete ring vortices will be formed in the jet issuing from orifice d_1 . When a vortex arrives at the second orifice, d_2 , a distance L away from d_1 , a pressure signal will be transmitted upstream, arriving back at d_1 after a time: $t_L = L/c$, where c is the speed of sound in the fluid. If the length, L , is selected as:

$$L = N\lambda = t_L V_c \quad (1)$$

where: λ is the wave length
 N is an integer number of vortices, and
 V_c is the vortex convection velocity, $V_c = f\lambda$,

then the pressure signal will arrive at d_1 at exactly the time required to excite a new vortex. Using the expressions for S_d and t_L , and introducing the Mach number: $M = V_1/c$, Equation (1) can be rewritten nondimensionally as:

$$\frac{L}{d_1} = \frac{N(V_c/V_1)}{S_d(1 + MV_c/V_1)} \quad (2)$$

Since $0.75 < V_c/V_1 < 0.5$, and $S_{d_1} = 0.3n$, the chamber length is determined for $M \ll 1$, by;

$$1.6 \frac{N}{n} \leq \frac{L}{d_1} \leq 2.3 \frac{N}{n} \quad (3)$$

The frequency of the cylindrical Helmholtz chamber, for large values of V/d_1 , is approximately given by the following equation:

$$f = \frac{c}{2\pi} \sqrt{\frac{\pi d_1}{4V}} = \frac{c}{2\pi d_T} \sqrt{\frac{d_1}{L}} \quad (4)$$

Thus the optimum diameter d_T for maximum amplification is given by the relation:

$$\frac{d_T}{d_1} = \frac{1}{2\pi S_{d_1} \cdot M} \sqrt{\frac{d_1}{L}} \quad (5)$$

which becomes after taking into account the inequality (3);

$$\frac{0.42}{M} \frac{1}{\sqrt{nN}} \leq \frac{d_T}{d_1} \leq \frac{0.66}{M} \frac{1}{\sqrt{nN}} \quad (6)$$

The ratio d_2/d_1 appeared experimentally to give optimum results at a value of 1.2 [17].

C. PULSER-FED SERVOJET

A self-resonating nozzle concept, which has been shown to be capable of providing several advantages relative to the PULSER SERVOJET, is shown in Figure 2. Shown are a basic design, Figure 3a, and two designs (3b, 3c) with alternative diffusion chambers. In this concept the exit nozzle, d_3 , is fed a fluctuating excitation by the same tandem-orifice with intervening resonant chamber configuration as described in the preceding section.

The advantages of the PULSER-FED SERVOJET concept have been shown to be:

a. The jet formed by the exit nozzle, d_3 , has a more uniform velocity distribution, and the vortices formed here are more cleanly defined.

b. The PULSER (d_1) nozzle can be selected to operate at a Strouhal number higher than that of the exit (d_3) nozzle. This implies that the resonant chamber pressure can be higher than p_a , the ambient pressure surrounding the jet exiting from d_3 , and that the velocity in the chamber is less than V_0 . Therefore, the cavitation number in the chamber will be much higher than that of the exiting jet, and cavitation in this chamber can be avoided.

c. The diffusion chamber (L_d, D_d) may be designed to enhance the amplitude of modulation provided by the PULSER chamber.

Disadvantages of the PULSER-FED concept include:

a. A more complex mechanical configuration, and

b. The overall energy loss, caused by losses in the

diffusion chamber, is greater than for the PULSER CAVIJET concepts.

The latter problem can be minimized by using the alternative diffusion chambers shown in Figures 3b and 3c. At any rate these losses are, by far, smaller than the losses in the presence of interrupting devices such as rotating discs or rotors.

d. ORGAN-PIPE SERVOJET

A SERVOJET concept which offers the simplest design, and was very successful for cavitating submerged applications is shown in Figure 2b. This concept achieves peak acoustic resonance when a standing wave forms in the "organ pipe" section (length: L_p , diameter: D). This section is created by the upstream contraction, $(D_p/D)^2$ and the nozzle contraction, $(D/d)^2$. Peak resonance will occur when the frequency of the organ-pipe wave is near the preferred jet structuring frequency. The exact resonance frequency is dependent on the contractions at each end of the organ-pipe. For instance, if both $(D_p/D)^2$ and $(D/d)^2$ are large, then the first mode resonance in the pipe will occur when the sound wave length in the fluid is approximately four times L_p . When the contraction ratio D/d is not too big, resonance occur when the wave length is approximately two times L_p .

The real design problem for an ORGAN-PIPE SERVOJET is the generation of the initial excitation of the oscillations in the organ-pipe chamber. This is successfully achieved in the submerged mode through a feed-back mechanism on the exit section of the nozzle. As discussed below, time has not allowed for such success for in-air application and further research is required to achieve this objective. Acoustic analysis and experimentation under submerged conditions have led to the

following approximation, useful for estimating the length of the organ-pipe:

$$\frac{L_p}{d} = \frac{K_n}{M S_d^*} \quad (7)$$

where the "mode parameter", K_n is given, for $D_F/D \gg 1$, by:

$$K_n = \text{func.} (n, \frac{D}{d}, M) = \frac{2n-1}{4} ; \text{ for } \frac{D}{d} \leq \sqrt{M} \quad (8)$$

$$= \frac{n}{2} ; \text{ for } \frac{D}{d} \geq \sqrt{M} \quad (9)$$

In these expressions:

- n = mode number of the organ-pipe,
- S_d^* = critical Strouhal number, $fd/V = 0.3 \times n$
- M = Mach number, V/c .

An empirical relation found useful for designing an ORGAN-PIPE CAVIJET is:

$$M = \frac{K_n}{S_d^*} \left[\frac{d}{L_p} - 0.86 \left(\frac{d}{L_p} \right)^2 \right] \quad (10)$$

If the feed-back can be achieved in non-submerged conditions, the same relation (7) is expected to remain valid but with different values of K_n and principally S_d^* . This comes from the fact that, first the acoustical impedance at the nozzle exit is not the same in the two cases and that, second, the shear stresses are much weaker in the non-submerged case and thus the critical Strouhal number is different.

III. OPTIMUM OSCILLATIONS FREQUENCY RANGE

We present in this section a preliminary analysis aimed at defining an optimum work region for the SERVOJETS. This analysis, to be refined and improved in future work, is essential to any attempt to optimize the cleaning or cutting rate of the train of slugs generated by a SERVOJET. The main parameter to be analyzed, besides the impact forces imparted to the impacted surface, is the optimum frequency of those impacts for an interrupted jets.

A. Stresses Due to a Point Load on an Infinite Elastic Medium

In order to obtain a rough estimate of the order of magnitude of the stresses imparted to the coatings we consider the case of a point load on an infinite, isotropic, homogeneous medium. We recognize that this model should be modified to account for the very finite thickness of the coating and for the presence of the substrate. However, in the idealized case of a perfect reflection of the stresses on the interface, the conclusions drawn below keep their validity.

In the infinite medium, the elastic stresses due to the point load, in a spherical coordinate system, depend on the load F , the Poisson's ratio ν , and the position of M (r , θ , ϕ), as follows:

$$\begin{aligned}\sigma_r &= \frac{F}{4\pi} \cdot \frac{\nu-2}{1-\nu} \cdot \frac{\cos \theta}{r^2} \\ \sigma_\theta &= \sigma_\phi = \frac{F}{4\pi} \cdot \frac{1-2\nu}{1-\nu} \cdot \frac{\cos \theta}{r^2} \\ \sigma_{r\theta} &= \frac{F}{4\pi} \cdot \frac{1-2\nu}{1-\nu} \cdot \frac{\sin \theta}{r^2}\end{aligned}\quad (11)$$

In these expressions the normal stresses σ_r , σ_θ and σ_ϕ are compressions when negative. $\sigma_{r\theta}$ is the shear stress.

For a given F , the relative importance of compression, tension or shear failure at a given point is seen to be dependent on v , and hence on the particular coating property.

Another observation derived from (11) relates to the importance of F on the volume in which failure would occur. Whatever criterion of failure one applies, the region in the coating in which the concerned stress exceeds some material strength, S , is of a length scale, r_ℓ , proportional to $F^{1/2}$:

$$S = k_1 \frac{F}{r_\ell^2} \rightarrow r_\ell = \left(\frac{k_1}{S}\right)^{1/2} F^{1/2} \quad (12)$$

Then if we assume that the removed volume, v_0 , scales with r_ℓ^3 , we can write:

$$v_0 = A(v, S) \cdot F^{3/2} \quad (13)$$

where A is a function dependent on coating properties. In the case we are interested in, F is the total force due to the impact of a continuous jet, or by extension to the unsteady case, the total force generated during the impact of a discrete water packet.

B. Impact Forces

It is known that the highest rate of erosion achieved with a continuous jet is obtained during the initial part of impact. Indeed, as in the case of a slug-structured jet, the initial force of the impact is proportional to ρcV , then drops rapidly to $\frac{1}{2}\rho V^2$. At any subsequent time the total force, F_c , applied by a continuous jet of diameter d , is:

$$F_c = \frac{1}{2} \rho V^2 \cdot \frac{\pi d^2}{4} \quad (14)$$

A much higher force is applied in the case of slugs of projected diameter, D , due to the water hammer impact, but is applied at intermittent periods:

$$F_s = \rho c V \cdot \frac{\pi D^2}{4} \quad (15)$$

The ratio between the two forces shows that the gain due to the interruption of the jet is inversely proportional to the Mach number, M (where $M = V/c$) of the jet and directly proportional to the ratio of the increased area of impact, A_1 , to that of the continuous jet, A_j .

$$\frac{F_s}{F_c} = \frac{c}{V} \cdot \left(\frac{D}{d}\right)^2 = M^{-1} \cdot \left(\frac{A_1}{A_j}\right) \quad (16)$$

The basic interpretation shows that, since $D > d$; (See Equation (22) below), and $M \ll 1$, by producing discrete water packets one can take advantage of impact forces an order of magnitude higher than in the continuous case to generate material failure.

C. Relations for Complete Bunching in a Modulated Jet

Nebeker [8] and Sami [18] have made a detailed analysis of the influence of the amplitude of modulation on the bunching process. A straight forward approach to the problem can be made as follows: Let V be the mean speed of the jet and $\frac{\Delta V}{2}$ the amplitude of speed modulation (Figure 4). If λ is the wavelength of the perturbation, a crest overtakes a trough after a time, T :

$$T = \frac{\lambda}{2 \Delta V} \quad (17)$$

The required distance to bunch is then:

$$X = TV = \frac{\lambda}{2} \frac{V}{\Delta V} \quad (18)$$

which can be expressed nondimensionally, relative to the jet diameter, d , as follows:

$$\frac{X}{d} = \frac{1}{S_d} \frac{1}{2\Delta V} \quad (19)$$

where S_d is the Strouhal number based on the jet diameter:

$$S_d = \frac{fd}{V} = \frac{d}{\lambda} \quad (20)$$

Equation (19) gives the distance needed for complete bunching for a given frequency and amplitude of modulation.

While moving, the shape of the water packet changes from cylindrical to spherical, and then to a disc shape before being stretched and broken into minute drops [19]. The diameter, D , of the spherical drop formed is given by:

$$\frac{\pi d^2 \lambda}{4} = \frac{\pi D^3}{6} \quad (21)$$

which can be written:

$$\left(\frac{D}{d}\right)^3 = \frac{3}{2} S_d^{-1} \quad (22)$$

This gives for $S_d \approx 0.3$, $D \approx 1.71 d$. Anno [20] reports a "generally accepted value" for D of about $2d$.

D. Optimum Frequency1st Criterion: Relaxation

In order to take advantage of reflections at the interface between two layers of coatings, or at flaws and weaknesses inside the coating to create stresses capable of generating failure, a certain time is needed between two impacts to let the energy be released. Due to losses of energy during the wave travel, the region close to the reflecting area is the most vulnerable. Therefore, the relaxation time has to be of the same order of magnitude as the pulse duration, T . And, since the high pressure following the impact of a drop of radius R has a duration of about $T \approx 2.5 R/c$ (see review in [19,21]), the frequency of impact has to be small compared to $1/T$. If we consider $f < 4T$, for example, we obtain by combining with Equation (22):

$$F \leq 0.2 \frac{c}{d} S_d^{1/3} \quad (23)$$

By introducing the jet Mach number, $M = V/c$, (23) becomes

$$S_d \leq 0.1 M^{-3/2} \quad (24)$$

Condition (23) should be made more accurate by introducing the coating thickness, δ , and the sound speed in the coating medium $c\delta$, and comparing T and $\delta/c\delta$.

2nd Criterion: Cushioning Effect

In order to prevent an important cushioning effect of the following impact due to the presence of a liquid layer on the target, a limiting time is needed between two impacts. This time is of the order of magnitude of the total time of crushing of one slug, and can be approximated by:

$$T_1 \approx 2R/V \quad (25)$$

The frequency of impact must therefore be smaller than $1/T_1$; and thus the Strouhal number is limited by:

$$S_d = \frac{fd}{V} \leq \frac{d}{2R} \quad (26)$$

Taking Equation (22) into account, (26) can be written:

$$S_d \leq 0.85 \quad (27)$$

With $V = 500$ ft/s and a $\frac{1}{2}$ -in. diameter jet, the frequency of modulation should be smaller than 6000 Hz.

3rd Criterion: Aerodynamic Effects

The aerodynamic effects are the principal limitations for any of the approaches presented above. Once it is formed, a drop or bunch cannot keep its integrity for a long period of time. The equilibrium between surface tension forces and aerodynamic drag forces is preserved as long as the Weber number:

$$W_e = \frac{2\rho V^2 R}{\sigma} \quad (28)$$

is not bigger than a limiting value (≈ 50). This limits the maximum stable drop diameter to a fraction of microns! However, the distance needed for rupture is several times R , so that if the target is close to the region where bunching starts the rupture can be avoided. In addition, drag forces can be reduced by trying to produce slugs with diameter, D , close to the jet diameter, d . This can be written:

$$\frac{D}{d} = \left(\frac{3}{2S_d} \right)^{1/3} \leq 1, \text{ or } S_d \geq 0.66 \quad (29)$$

which gives a frequency higher than 4000 Hz for the $\frac{1}{2}$ -in., 500 ft/s jet.

The preliminary criteria developed here are summarized in Figure 5, in which the "optimum" working region, obtained by application of these criteria, is shown. This optimum region is a narrow one: $0.66 \leq S \leq 0.85$, and is based on a preliminary analysis. It is intended for guidance only. The actual optimum range is probably broader and centered around 0.75, say 0.3 to 1.2.

E. Comparison With Existing Studies

In his study, Nebeker [8] reports frequencies of the oscillations between 12,000 and 20,000 Hz, with nozzle diameters of 0.06 and 0.08 inches, and pressures across the nozzle of order 7,200 psi. Although the values of the frequencies are not too precise, the maximum and minimum values of the possible Strouhal numbers ($S = fd/V$) of the flows investigated in Reference [8] can be estimated to be: $0.06 \leq S_d \leq 0.12$.

A similar interpretation of the Erdmann-Jesnitzer [5] results shows that, with frequencies of 500 Hz and 2500 Hz, the Strouhal number was between 0.002 and 0.01. The same range of Strouhal number is investigated by Janakiram [6] showing constant increase in cutting rates with increasing S_d .

As we can see, these numbers are much smaller than the optimum ones proposed above. As a result, although these studies showed large improvements in cutting rate with increasing frequency, their Strouhal numbers were always too small to identify the existence of an optimum frequency.

IV. EXPERIMENTAL FACILITIES AND TECHNIQUES USED

A. Facilities

All the tests described in this report were performed in the largest test chamber established at HYDRONAUTICS for CAVIJET studies. This chamber is 1.8 m long, 1.5 m wide and 1.8 m high and can be used for tests either on submerged materials or in air. A hydraulic translator allows the jet to be translated at any velocity up to 1.2 m/s across the material being eroded.

In order to avoid a water-layer formation during the cleaning tests, which could cushion the slug's impact, this chamber was modified to allow the nozzles to be positioned horizontally at one end of the chamber while the target was positioned vertically at the other end. Vertical guide rails were installed and a specimen holder designed and built. A system of pulleys enabled the transmission of the horizontal motion of a hydraulically moved piston to the vertically guided specimen holder. The nozzles were fixed to a movable (x-y) carriage whose variable position fixed the stand-off distance between the nozzle and the panels. In order to facilitate the visualization of the jet behavior, a splash-absorber consisting of a solid wall, with an aperture slightly bigger than the expanded jet diameter, was placed in front of the panel-target. For pictures and high-speed movie taking purposes, however, we found it easier to shoot the jet vertically to the bottom of the tank covered with a water layer of a few inches. We succeeded very effectively in eliminating splashes and water spray by a splash absorber laid above the free surface of the water.

The facility includes (in addition to the tank) pumps, reservoirs to recover and store the working fluid, suitable filters, controls and gages for pressure and temperature, and

flow measuring devices. The pumps used were all of positive displacement design. Driven by a 75 kw (100 hp) motor is a 303 ℓ/m (80 gpm) capacity triplex, with a maximum pressure rating of 15.2 MPa (2,200 psi). A diesel-driven, portable quintuplex, with various sets of plungers, allows a range of flow and pressure combinations in any pairing within the 112 kw (150 hp) power-envelope from 341 ℓ/m (90 gpm) at 1.7.2 MPa (2,500 psi) to 76 ℓ/m (20 gpm) at 68.9 MPa (10,000 psi).

In addition to this installation, an air-test facility was used to rapidly evaluate the characteristics of various self resonating chambers. A rectangular plenum supplied air to the device being tested. The pressure in the plenum was controlled with a needle valve in the 0.2 MPa (20 psi) air supply line and was monitored with a U-tube manometer. Flow from the test nozzle discharged to the atmosphere. Perturbations in the jet's axial velocity were surveyed with a 25 μ diameter hot wire sensor. The detected signal was electronically processed. The raw voltage signal from the Thermo-Systems Inc. (TSI Model 1050) hot-wire anemometer bridge was fed directly to a TSI Model 1060 RMS Voltmeter, a spectrum analyzer (Hewlett Packard 3580A), and an X-Y plotter. The mean and the root-mean-square anemometer voltages can be continuously recorded. The spectrum analyzer output, viewed on an oscilloscope, or recorded on the X-Y plotter, permits the detection of resonant frequencies in the perturbation velocity; these are manifested as sharp spikes or peaks in the spectra.

The other instruments and equipment used for this project are high-frequency response pressure transducers (PCB Piezotronics, ICP Model 101A04, resonant frequency 400 kHz), a high-speed camera, HYCAM, capable of 10,000 frames per second (or 40,000 quarter frames per second), various still motion cameras,

a laser, a photo multiplier and a signal amplifier.

B. Techniques for Bunching Detection

Three ways of detecting the effective bunching of the jet in discrete packets were used; two of them were optical and the third acoustical. High quality visual observation of the phenomena is the most reliable and the most comprehensive way for studying the bunching characteristic both quantitatively and qualitatively. High intensity, low duration (30 μ s) flash pictures were taken. This method was satisfactory up to a jet velocity of 300 ft/s. At higher velocities, the exposure time became too long relative to the time scale of the phenomenon, resulting in streaky and blurry pictures.

Another direct method of detecting the bunching of the jet consisted of using a piezoelectric transducer protected by a layer of hardened epoxy as a direct target for the jet, or a measuring device of the pressure transmitted through a pin-hole drilled in a metallic target. While a continuous jet gave a reasonably flat output signal a pulsed jet signal was characterized by spikes at constant time intervals corresponding to the oscillation frequency. A frequency analysis of the amplified output of the transducer proved to be a satisfactory means of detecting the presence or not of discrete frequencies, and thus of bunching, in the jet. Unfortunately the use of transducers as direct targets seems to be (at least in the way we performed the tests) a poor and rather expensive idea. The passively generated slugs apparently produce shock waves high enough to destroy probes capable of a nominal pressure of 10,000 psi (PCB Piezotronics, ICP Model 101A04). After destroying two probes, we stopped using this technique. The use of the transducer fitted under the target and communicating

with the impacting jet by means of a pin-hole presented no difficulties. Another transducer flush-mounted inside the straight tube of length L (Figures 2 and 7) was successfully used to correlate the pressure fluctuations and their characteristic frequencies with those measured in the jet itself.

The second optical method proved out to be the fastest and the most practical: a laser beam was shone through the jet; the transmitted beam of light was amplified by a photo multiplier (PM) and the signal analyzed. In the absence of excitation and at lower stand-off distances the jet is continuous and little light crosses to the PM. At greater stand-off distances the jet integrity is destroyed and the PM signal looks very random. However, when the jet is excited the laser beam is periodically interrupted by the existing slugs. In this case the signal displays a characteristic periodicity, and its frequency spectrum correlates highly with the pressure transducer signals and the slug pictures as shown below. Figure 6 summarizes the experimental set-up described above.

C. Tested Nozzles

Before we made the final choice of the nozzle shapes to test for this study, the performance of several existing nozzles was observed. These nozzles were developed earlier at HYDRONAUTICS in order to increase the erosive capabilities of submerged jets by enhancing cavitation in the shear layer. Both PULSER and PULSER-NEED (Figure 2) configurations were tested and compared with the behavior of the same nozzles in the absence of the Helmholtz chambers, all other dimensions and flow conditions being comparable. Single flash pictures of the jets showed a radical change in their appearance. The free surface of the nonexcited jet looked smooth and stretched, but these jets were diverging substantially. The excited jets

exhibited bunching characteristics but were spreading out very early, a few jet diameters downstream of the exit. In these preliminary tests we did not pay any attention to the inlet conditions, the smoothness of the flow and the nozzle shape. Based on these observations, it seemed fundamental to design a nozzle capable, in absence of excitation, of attaining a large stand-off distance before starting to spread. A survey of the literature confirmed the great influence of the inside contour of the nozzle on the maximum reach of the jet. A CAVIJET shape with a contour closer to an ellipse rather than to a circle should give the greater reach even when compared with the well-known Rouse shape [22]. As time would not have allowed for systematic research on inlet contours, we chose an elliptical CAVIJET shape similar to the one selected in a recent review article on the subject [22]. A Leach and Walker nozzle was also used for comparison purposes.

In order to generate comparable data between the various configurations tested, the nozzle assembly represented in Figure 7 was constructed. For a given inside shape of the nozzle, the lip thickness, e , could be changed by replacing piece B. This also allowed testing various contours of the nozzle shape. The jet was excited either by inserting piece A in Figure 7 (PULSER-FED configuration) or by the correct choice of e and the outer contour of the lip in order to provide a feed-back mechanism to the organ-pipe of length, L . In absence of piece A and when e is zero we have our basic plain CAVIJET with a long e we obtain an ORGAN-PIPE nozzle and when A is present we generate a PULSER-FED nozzle. A jet would be nonexcited both when part A is removed and e is zero or the nozzle has a classical shape (e.g., Leach and Walker nozzle).

In order to be able to generate a controlled excitation

corresponding to the resonance characteristics of the system, the ratio D_1/D_2 (Figure 7) was chosen big enough to ensure a great variation of the acoustical impedance at the inlet section of the nozzle. This condition limited the highest value of the jet diameter to 0.185 inches for a maximum pressure drop across the nozzle of 2,000 psi. Bigger diameters can be studied in future work at these pressure provided that a modification is made to the diameter of the feed tube.

Another important condition for a good control of the acoustical behavior of the jet is a "clean" long straight inlet tube of diameter D , upstream of the nozzle. A tube 11.5 inches long was used for all configurations tested. Its diameter was 1.3 inches for ORGAN-PIPE and PULSER-FED SERVOJETS and 0.53 inches for nonresonating jets. The diameter, D_2 , of the exit tube was also 0.53 inches and its length was 4 inches.

As we discuss below two series of nozzles were used. The first was designed for low velocities and allowed assessment of the validity of the measurement techniques and characterization of the jet flow oscillations. The design of the second series was based on the knowledge acquired from the first nozzles and considered higher pressures to enable paint and coating removal. Due to the flow rate limitation of the pump, smaller jet diameters were imposed as well as related changes in the resonating chambers.

For visualization and techniques evaluation purposes the Helmholtz resonator chamber and the organ-pipe characteristics were chosen to give optimum performances at a Mach number of 0.1, which corresponds to a value of $\Delta p \approx 1600$ psi. Based on the equations presented in Section II, this corresponds to the dimensions: $d_1 \approx 0.23$ inches, $d_2 \approx 0.28$ inches, $d_T \approx 0.79$ inches and $\rho \approx 0.37$ inches. The nozzle shapes investigated were an elliptical

CAVIJET shape (Figure 8) with lip thickness $e \approx 0.02$ inches and $e \approx 0.23$ inches, and a Leach and Walker nozzle (Figure 9).

The exit diameter of the Leach and Walker nozzle of 0.155 inches was calculated in order to compensate for the higher coefficient of contraction of the CAVIJET nozzle. Both the CAVIJET nozzle of diameter 0.185 inches and the Leach and Walker nozzle of diameter 0.155 inches produce the same jet velocity for a given discharge.

For paint cleaning purposes two new nozzles were designed and fabricated: a CAVIJET shape nozzle (0.1 inch diameter) (Figure 8) and a Leach and Walker nozzle (0.084 inch diameter) (Figure 9). Smaller diameters than the earlier design were chosen to enable a pressure drop across the nozzle as high as 10,000 psi with a pump capable of 20 GPM. The same resonating chamber as described above was first used to study nonmatched acoustical conditions. A more adapted chamber was then constructed: $d_1 \approx 0.16$ in., $d_2 \approx 0.19$ in., $d_T = 0.34$ in., and $l = 0.25$ in. In an effort to generate feed-back at the nozzle exit for ORGAN-PIPE oscillations, several lip thicknesses, e , were studied. We report below on three values $e \approx 0.20$, 0.13, and 0.08 in.

V. EXPERIMENTAL RESULTS

A. Flow Corrections

In order to make justifiable comparisons between the different nozzles used, two corrections were applied. The first one dealt with two nozzles of different shapes (i.e., CAVIJET and LEACH & WALKER) and thus of different discharge coefficients. These discharge coefficients were determined using the air facility and, as stated before, the diameter of the LEACH & WALKER nozzle was chosen smaller in order to compensate for this difference. With the final choice the LEACH & WALKER nozzle had the same flow rate and the same jet velocity as the corresponding CAVIJET for a given pressure drop across the nozzle.

The second correction was concerned with the losses introduced by the presence of the PULSER-FED Helmholtz chamber in the feed-tube of the nozzle. The air facility was used to determine the discharge curves (Figures 10 and 11) for the considered nozzles, with and without the Helmholtz chamber. A comparison between the two curves allowed for an equilibration of the total pressure drop across the two compared nozzles in order to obtain the same exit velocity. For the low velocity, larger diameter first series of jets (SERVOJET, $d \approx 0.185$ in., LEACH & WALKER, $d \approx 0.155$ in.) Figure 10 presents the discharge curves and shows the presence of losses as high as 24 to 28 percent. A mean value of 26 percent was used in subsequent tests. To obtain the same jet velocity one has to use a pressure drop across the nozzle assembly 26 percent smaller for an ORGAN-PIPE or a plain jet than for a PULSER-FED jet.

As can be seen in Figure 11 the losses were substantially smaller for the second series of jets — high velocity, smaller diameters (SERVOJET, $d \approx 0.1$ in., LEACH & WALKER, $d \approx 0.084$ in.)

A mean value of six percent correction was applied in all of these tests. The oscillatory behavior of the discharge curve is very interesting to notice and can be related to later discussions on ORGAN-PIPE SERVOJETS in this report. Indeed, these oscillations are directly related to an ORGAN-PIPE resonance of the nozzle assembly even without the Helmholtz chamber. The pressure fluctuation curves in the upper part of Figure 11 show the intensity of these oscillations. However, this did not alter our tests since the ORGAN-PIPE SERVOJET nozzle which was studied had produced highly structured resonating air jets in the submerged condition: air-air, while it was very poorly structured in the nonsubmerged conditions: water-air (see Figure 26).

B. Photographic Evidence

We highlight in this paragraph the observations we have made concerning the appearance of water-in-air jets in the presence and in absence of self-excitation. We will present pictures obtained with a single flash lighting with a NAMIYA camera and Kodak 4X black and white films. We also took some infra-red pictures in an effort to minimize the influence of the mist surrounding the jet. However, in the pressure range over which we tested, this technique did not show a noticeable advantage. Three high-speed movies of the jet with the HVCAM were exposed, but the picture quality of the still pictures was better because of the shorter exposure time of the flash relative to the shutter speed of the HVCAM.

Figure 12 shows the oscillations and production of droplets for jets of relatively low speed. The first case (Figure 12a) illustrates the phenomenon of jet breakup by the Rayleigh instability. The two other pictures show the dynamical instability [19-20] which is followed by the rupture of the jet into slugs. Here the velocity is still relatively low so that air entrainment

and mist production do not affect the jet's appearance.

Figures 13 and 14 compare, at two different velocities, the structure of a self-oscillating jet with that of a nonexcited jet obtained with the same nozzle. For all the jets seen in these figures the same Leach and Walker exit nozzle was used. The only modification between the oscillating and nonoscillating configurations is the existence of the resonance chamber in the former (piece A, Figure 7). The presence of discrete structures or "packets of water" is clearly observed for both values of the pressure drop, Δp , across the nozzle assembly (600 and 900 psi) for the SERVOJETS. As the dominant frequency is practically the same in the two cases (4 kHz), the distance between the slugs is seen to increase with V . Here, as often observed for several studied configurations, a subharmonic ($0.15 \leq S_d \leq 0.2$) to the known fundamental jet turbulent frequency ($S_d = 0.3$) for submerged jets, is present. This is due to the fact that for these nozzles ($d_1 = 0.23$ in., $d = 0.185$ in.) the Strouhal number based on the upstream conditions, S_{d_1} (i.e., on the jet issuing from d_1) is twice as big as S_d . We have thus the more usual result ($0.3 \leq S_d \leq 0.4$). Another factor which needs more investigation is the value of the predominant Strouhal number of the nonexcited water-in-air jet which, as we discuss below, is not the same as for a submerged jet. The bunching frequency based on the distance between two slugs and the jet velocity matches perfectly, within the accuracy of error measurements, the frequency inside the tube. As an example, Figures 13b, 14b, and 14c give a frequency of 3.75 kHz while the measured dominant frequencies in the tube are 4 and 3.8 kHz.

The next two Figures, 15 and 16, show the case of well structured PULSER-FED SERVOJETS with a CAVIJET nozzle. Very distinct structuring is observed as well as a "fanning" of the

slugs due to air drag. Figure 15 corresponds to the low-velocity, larger-diameter nozzle in its optimum working region (maximum oscillation). Figure 16 corresponds to the smaller-diameter nozzle in its first peak of oscillations (see Figure 25, $M = 0.07$). In both figures the following description of the modulated jet applies: first, "bulbs" appear in the core; next, the bulbs are detached into slugs; and then they become greatly deformed due to air drag. The maximum energy of impact is obtained just in the detachment region, while cleaning rates indicate higher efficiency in the "fanned" region.

C. Pressure Fluctuation and Laser Beam Interruption

As described in Section IV, paragraph B, and sketched in Figure 6, a pressure transducer used as a target and another one installed in the nozzle tube allowed measurement of the acoustical properties of the oscillations. Another direct technique to detect the bunching characteristics of the jet was based on interrupting a laser beam and analyzing the transmitted light variations with time. We present here the results of these measurements.

Figure 17 shows the frequency spectrum, for the nonexcited jet (CAVIJET shape, Figure 10, with $d = 0.185$ in., $e = 0.02$ in.), of the pressure oscillations at the location of the pressure transducer in the feed tube. This spectrum did not change when changing the length of this tube and seemed to arise from a feed-back mechanism from the jet oscillation back to the tube (see next section D). Let us note, however, that the relative amplitude of the oscillations, $p'/\Delta p$, is only 0.4 percent.

Figure 18 presents, for the same jet exit velocity as in the preceding figure ($V = 360$ ft/s), the noise frequency spectrum for the self excited jet. These self-oscillations are induced by inserting the Helmholtz chamber in the nozzle assembly

(Figure 7). (The pressure drop across this nozzle assembly is increased to compensate for the losses and to obtain the same jet exit velocity.) Here, the frequency peaks are very sharp and discrete and the pressure fluctuations are an order of magnitude higher than for the plain jet ($p'/\Delta p \approx 5.2\%$). The locations of the frequency peaks are a result of the choice of the geometry of the pulser chamber. It was designed to function at a Strouhal number, S_ℓ , based on the chamber length, which is a multiple of 0.3, and to resonate (give maximum amplification) at $\Delta p = 1600$ psi, and a Strouhal number, S_{d_1} , based on the upstream diameter d_1 (see Figure 7) of value 0.5. Due to this particular choice we have $S_\ell \approx 3 S_{d_1}$, and the three observed peaks happen to be at $S_\ell \approx 0.36, 0.60, \text{ and } 0.96$ which correspond to the first, second, and third mode of the pulser chamber (presence of 1, 2, or 3 ring vortices between orifices d_1 and d_2).

Figures 19 and 20 show, for approximately the same jet velocity, ($V \approx 210$ and 205 ft/s) how the frequency spectrum of the pressure signal in the nozzle tube strongly correlates with the spectra of both the impact pressure oscillations on a transducer-target (Figure 19) and the modulation of the laser beam interrupted light (Figure 20). This result is very encouraging for future studies since one of these measurements is sufficient and gives the needed information on the frequency concerning the two others. This correlation between optical and acoustical observations was used for the remainder of the study, to generate high pressure self oscillating jets. Another observation from Figure 19 is that the pressure fluctuations are largely amplified between the pipe and the optimum distance ($X = 7$ in.). A multiplication factor of four has affected the value of $p'/\Delta p$. We also observe that this optimum standoff distance corresponds to the one predicted by Equation (19). Indeed, with

$$\frac{p'}{\Delta p} \approx \frac{\Delta V}{V} = \frac{1}{2} \cdot \frac{d}{X} \cdot \frac{1}{S_d} \quad (30)$$

(p' : amplitude of pressure oscillation, ΔV : double amplitude of velocity oscillation), the needed pressure oscillation to obtain $X = 7$ in. and $S_d \approx 0.33$, with $d = 0.185$ in. is:

$$p'/\Delta p \approx 0.04, \quad (31)$$

which is very close to the pressure oscillations measured in the pipe (3.5%).

In Figure 21, the pressure oscillations in the tube are compared with those sensed by a transducer fitted in a flat plate and used as a target. The frequency spectra at four different standoff distances are compared. An excellent correlation between all these spectra can be seen. Some differences can, however, be observed. First, the harmonic, $f \approx 3.1$ kHz, $S_d \approx 0.20$ which exists in the tube has practically disappeared in the jet itself. The self-oscillations of the system have selected the main turbulence frequency of the jet, $f \approx 5.5$ kHz, $S_d \approx 0.38$. However, the second harmonic and, to a lesser extent, the third harmonic which are very weak inside the tube are strongly amplified in the jet. Figure 21 also gives valuable information on the structure of the jet and on its "aggressivity" at various standoff distances, X . At too small or too large distances from the nozzle exit the impacting pressure oscillations, as well as the energy content of the main frequency, are relatively low. In the present case, the shape of the nozzle is a CAVIJET shape, with $d = 0.185$ in., $V \approx 220$ ft/s, and the pressure fluctuations observed, $p'/\Delta p$, were 2.2% at $X = 1$ in., and 2.0% at $X = 15$ in. The optimum standoff distance in this case appears from these measurements to be at $X \approx 7$ in. ($X/d \approx 38$) where $p'/\Delta p \approx 10\%$, for pressure fluctuations inside the tube of only 2.5%.

Figure 22 shows a correlation between the frequency spectra of the laser transmitted light signals at two different distances, X , from the nozzle exit, and the spectrum of the pressure fluctuations inside the tube. A perfect correlation in the position of the peaks can be observed. Here, the subharmonic of the main frequency (7.1 kHz, $S_d \approx 0.37$) is predominant in the pipe oscillations. This predominance is also reflected in the slug formation and thus in the interrupted laser beam signal. The structuring is observed to have ameliorated between the two inspected locations $X = 10$ in. and $X = 16$ in.

The use of pressure transducers as direct targets for the oscillating jets was limited to a jet velocity of 320 ft/s ($\Delta p \approx 700$ psi). The water-hammer pressure due to the impact of a slug at such a speed is approximately 23,000 psi. Even with a shock absorption factor of two this pressure exceeds the limiting dynamic pressure of the transducer which is 10,000 psi. The laser interruption technique, however, does not have the intrinsic limitation of the pressure transducer technique. The only limitation for the laser arose from practical reasons related to the use of the tank. This tank was covered in order to reduce environmental noise; during a test run it became foggy and water condensation droplets obscured the PM view. The system worked satisfactorily up to a jet speed of 350 ft/s. Above this speed only diffuse light with white noise (very broad frequency content) passed through the PM amplifier. The same type of spectrum was obtained with a plain nonexcited jet. This was the case for all the jets tested (Leach and Walker, ORGAN-PIPE, $e \approx 0.02$ and $e \approx 0.032$ in.) in the absence of a Helmholtz chamber. This fogging problem can be alleviated by working in an open tank or outdoors. The use of a metallic plate with a drilled pin hole, as a protective means for the transducer, worked out very satisfactorily for jet pressures as high as 10,000 psi. This

technique was mainly used to explain the results obtained with paint cleaning and is presented below.

D. Acoustical Study of the Various Jets

1. PULSER-FED SERVOJET

As stated above the upstream Helmholtz chamber in the nozzle assembly was very successful in generating noticeable oscillations in the feed tube to the nozzle and thus discrete structuring of the jet into organized slugs. We present here some evidence and validation of the physical approach presented earlier (Section II.b), in order to explain the PULSER-FED mechanism. We will see mainly from the three cases presented that the oscillations are controlled by the jet oscillations in the upstream section at the entrance of the Helmholtz chamber (Figure 7) and that the amplitude of the oscillations is maximized when the generated frequency (which varies with the velocity, S_d remaining constant) matches the characteristic frequency of the Helmholtz chamber.

In Figure 23 we can see two parallel plots of the relative amplitude of oscillations, and of the Strouhal number of these oscillations, for the PULSER-FED chamber used for the low-velocity larger-diameter jets used for visualization purposes ($d \approx 0.185$ in., $d_1 \approx 0.23$ in., $l \approx 0.37$ in.). The variations of $p'/\Delta p$ and S_d , S_{d_1} can be seen for different jet velocities (the correct nondimensional parameter is the Mach number, $M = V/c$). We observe here, as for submerged jets [23,24], two different behaviors depending on the Reynolds number. For $R_e = Vd/\nu$ less than 5×10^5 , the Strouhal number is velocity dependent. At the lower Reynolds numbers an interaction mechanism exists between the large structures in the jet and the small vortices in the shear layer. The critical value of R_e is based on "whether or not transition to turbulence occurs in the nozzle boundary layer or in the initial free shear layer" [24]. At the higher Reynolds numbers the

Strouhal numbers are practically independent of the jet velocity and take on the mean values $S_d \approx 0.14, 0.22$ and 0.35 . This shows that the PULSER-FED SERVOJET is automatically tuned with the jet velocity and that its frequency is linearly dependent on this velocity. The strongest mode seems to be the second mode for the low Reynolds number region and either the second or the third mode for the higher R_e region. Let us notice again that the values of S_{d_1} , which are related to S_d by the relation:

$$\frac{S_{d_1}}{S_d} = \left(\frac{d_1}{d}\right)^2, \quad (32)$$

have in this case values twice as big as S_d , and since in the Helmholtz chamber the jet is practically in a submerged condition, the values of S_{d_1} are the usual ones of 0.3 and its multiples.

The optimum frequency of the Helmholtz chamber, as given by Equation (4), which is here 7.4 kHz, corresponds to a Mach number of 0.063 in the second mode ($n = 2$). As we can see in Figure 23 this corresponds to the optimum value of $p'/\Delta p$.

Figure 24 shows again the variation of $p'/\Delta p$ and S_d versus the Mach number, M , for the smaller diameter jet, $d \approx 0.1$ in., but with the same Helmholtz chamber. Here again the Strouhal numbers based on d_1 are close to 0.3 and its multiples, while the amplification of the oscillation is relatively very small (an order of magnitude lower than in the preceding case). This comes from a mismatch between d_1 , d_2 and d . Figure 25 shows how this amplification can be greatly improved by redesigning the Helmholtz chamber. In this figure, based on the equations in Section II.b, d_1 was reduced to 0.159 in., $d_2 \approx 0.19$ in., and $l \approx 0.255$ in.; however, no attempt was made to optimize the chamber. Again the same remarks apply concerning the Strouhal number based on S_{d_1} . This number was twelve and a half times S_d

in Figure 24 and is here (in figure 25) reduced to four times S_d . More research needs to be done on the optimization of this ratio, chosen arbitrarily here. The three peaks in the pressure oscillations were picked for comparative paint removal tests.

2. ORGAN-PIPE SERVOJET

The feed-back mechanism seems to be extremely hard to achieve in the water-in-air case. Two different sizes of e (Figure 7) were tested for the larger-diameter nozzles ($d = 0.185$ in.) and as discussed above only very small oscillations (0.4%) could be achieved in the nozzle tube. More surprisingly, the frequency of these oscillations was independent of the tube length. More tests were conducted for the high-velocity small diameter-nozzles ($d = 0.1$ in.) and the results are summarized in Figure 26. Three values for the lip thickness, e , are shown and the amplitude of oscillations (maximum 0.55%) versus Mach number are presented. One can see that the effect of e is very small, which implies that strong oscillations through feed-back have not yet been achieved.

Another striking factor is the constancy of the frequency emitted. Several peaks exist in the spectrum at the constant frequencies 3, 4, 10, and 11 kHz. These frequencies are independent of the jet velocity and of e . This suggests that the only noise fed back in the nozzle is a jet noise which might be organized through acoustic triggering and not vortex transport, as was discussed earlier. In this case the "Strouhal number" to consider would be based on the speed of sound (rather than the jet velocity) and would remain constant relative to the Mach number. This idea is reinforced by the oscillations detected in the Leach and Walker nozzle which are of the same order as those in the supposed ORGAN-PIPE nozzle, and have in addition the same frequencies. Since further research on the nozzle

shape was beyond the scope of the present effort, we considered only PULSER-FED nozzles for the following part of the program.

E. Paint Removal Tests

We performed all the self-resonating jet paint removal tests with the PULSER-FED SERVOJET, $d \approx 0.10$ in., and compared these results with the corresponding LEACH & WALKER nozzle, $d \approx 0.084$ in. All the tested panels were provided by the North Island Naval Air Station, in San Diego, California. The aluminum panels were actual aircraft panels with MIL SPEC coatings.

The graphite-reinforced plastic panels, which had an epoxy primer and a polyurethane top coat, were tested in our modified large test chamber. The panel edges were protected with a glass-reinforced adhesive tape to minimize water penetration under the unprotected edge. This water intrusion tends to delaminate and damage these panels. Each test panel was first mounted on a metallic plate, then placed vertically and transversed at a constant velocity perpendicular to the impacting jet. Several pump pressures and standoff distances between the nozzle and the panel were tested. Paint removal started to occur on these panels when peak pressure oscillations were achieved (see Figure 25) at translation velocities of 0.5 in./s for the first effective peak ($\Delta p \approx 3,420$ psi) and 1.5 in./s for the second peak ($\Delta p \approx 5,220$ psi).

The test plan involved investigating this second peak, by running a series of various standoff distances at a fixed translation velocity and thus determining the optimum standoff. This was repeated for both the SERVOJET and LEACH & WALKER nozzles, in order to make comparisons at the optimum performances of each nozzle. Unfortunately we discovered after a few tests that this objective could not be obtained with the originals panels we had received from the Navy, due to large nonuniformities in the

erosion strengths of both the paint and the carbon-reinforced plastic substrate.

Figure 27 clearly illustrates these nonuniformities. Comparing cleaning paths 1 and 3 one can see that while 3 is run at a higher translation velocity for the same speed of the PULSER-FED SERVOJET the panel was badly damaged. Run 1, which would be expected to be a more damaging test, has a very clean path wherein both the top coat and primer have been removed with no damage to the substrate. The same type of discrepancy can be seen again between Runs 4, 5, and 3.

Figure 28 shows another example of the difficulty of interpreting any results with these panels. A consistent pattern is seen between Runs 1, 2, and 3: increase of Δp and a corresponding increase of cleaning width. However, Runs 1 and 5, 2 and 6 which are at the same conditions show great differences in the cleaning rates. On this same panel a Leach and Walker nozzle at the same Δp cut through the panel at the extreme right end of the photograph. To give an indication of the cleaning rates Runs 3 and 7 correspond to a rate of about 15 ft²/hr.

Fortunately the aluminum panels seemed to be more consistent and the tests were repeatable, at least on the same panel. Important differences existed, however, between the several panels. Indeed, panel V for example (Table 1) had three MIL-C-83286 polyurethane-based coatings above the yellow MIL-P-23377 epoxy polyimide primer: a gray top coat of about 50 μ thickness, two silver coats tan 100 μ thickness and silver 50 μ thickness. Panel VII, had the same number of coats but the yellow "primer" was on top of the silver coat. Panel VI had just two coats: a grey top coat and a yellow primer. The results and the conditions for the path cleanings on these three panels are summarized in Tables 1 to 3. We will describe and interpret below some of these

results, concentrating mainly on panel V (Figures 29 to 32).

Figure 29 gives an overall view of the whole panel. The numbers written near each path correspond to Table 1, where the test conditions are presented. All the cleaning paths on this panel were performed at the same jet velocity, namely a pressure drop across the Leach and Walker nozzle of about 5,100 psi and a slightly higher (+6%) Δp for the PULSER-FED SERVOJET, to compensate for pressure losses in the Helmholtz chamber. The same translation velocity was considered in all cases, 1 in./s, and the main variable was the standoff distance, X. Visually, the optimum standoff distance for the PULSER-FED SERVOJET was determined to be about 14., but a more careful analysis of the cutting rates showed it to be at a higher value of X. To determine the optimum standoff for the Leach & Walker nozzle another panel, VI was used. A value of X close to 10 in. was obtained. A few other runs were made for confirmation on panel V, and a value closer to 13.5 inches was obtained (see paths 3C and 8B in Figure 29). Figure 30 compares the two nozzles when the standoff distance varied between 11 and 23 in. The PULSER-FED nozzle is seen to give a more uniform, wider path. A close look shows also that the removal rate of the third coat (see Figure 33) is in this case almost four times greater. Figure 31 shows very clearly this advantage of pulsing the jet when one compares the two paths 8B and 3C, both taken at the apparent optimum standoff distance of 13.5 in. Figure 34 shows two photomicrographs of the coating appearance in the jet cleaned path. While picture 34b shows a clean yellow primer, slightly pitted, in the case of the PULSER-FED SERVOJET, picture 34a shows the remainder of the third coat in the LEACH & WALKER case.

Figure 32 shows the same results as above for several stand-off distances. As examples paths 3B and 1A, which cleaned with

a PULSER-FED CAVIJET, have better cleaning rates than path 2A which is a PULSER-FED LEACH & WALKER or than path 3A which is a plain LEACH & WALKER. All four runs were at a 5 in. standoff distance. The same applies for paths 5B and 4A, with standoff distances of 8 and 10 in. respectively.

Figure 33 summarizes all the data from the panel V, (Table 1). In this figure we have presented the cleaning rate in ft^2/hr versus the standoff distance. The following method was used. The width of each coating removed was measured and an empirical percentage value, estimated by the same person, was attributed to the cases where partial removal of a coating layer took place. The surface cleaning rate for each coat was then calculated as the product of the width by the translation velocity by the affected removal percentage. The top coat was in all cases totally and easily removed in the total width for the pressures considered (SERVOJET, 5,400 psi, $d \approx 0.10$ in.; LEACH & WALKER, 5,080 psi, $d \approx 0.084$ in.). The removal rate was slightly higher for the SERVOJET over the entire standoff range, and seemed to peak at 12 in. Both nozzles had, however, the same cleaning rate with regard to the second coat up to $X = 12$ in.; then the oscillating nozzle became more effective. The most significant and interesting result concerns the final coat where a definite advantage can be seen for the PULSER-FED nozzle. A factor of three can be observed for $X \approx 15$ in.

We performed some preliminary tests to measure the impact pressure generated across the nozzle, in order to explain these results as well as some others as seen in Table 3. On this panel, where only two coats were applied, the cleaning rate of the LEACH & WALKER (at 5,080 psi) was much higher than the PULSER-FED at 5,400 psi. However, this result was reversed when the pressure was slightly increased. This seems to indicate

that the threshold of paint removal was not attained for the SERVOJET for the lower A_p and thus the cleaning rate was negligible. Once this threshold was passed the oscillations dramatically increased the erosion rate.

The pressure measurements involved moving the metallic target with a pin hole and a transducer in front of the jet and measuring the variation of the impact pressure with the radius, for both jets. Two comparative profiles are shown in Figure 35 for both jets. The two upper profiles correspond to the optimum cleaning rate case presented above (Figure 31). Surprisingly, the maximum pressures are much higher for the LEACH & WALKER than for the PULSER-FED nozzle, while the erosion rates are the opposite. A probable explanation is the fact that in one case the impacts are rather random, while in the excited nozzle case discrete frequencies of 10 and 25 kHz are present -- which create stress amplification in the coating. This requires more understanding and is a key element for any future development of the self-resonating cleaning jets.

VI. CONCLUSIONS

We have demonstrated in this work the feasibility of passively inducing self oscillations in a nonsubmerged water jet for paint removal applications. Two systems were investigated:

a) the insertion of a Helmholtz resonator upstream in the feed tube leading to the nozzle; PULSER-FED SERVOJET.

b) the generation of organ-pipe resonances in the nozzle tube through a feed-back mechanism at the nozzle exit.

The first system was very successful in achieving the jet structuring and results related to this system are thoroughly described in this report. The second system was less successful due, in our opinion, to lack of time available for researching an adequate exit shape. Similar research done at HYDRONAUTICS on submerged jets has shown great success in achieving high levels of self oscillations; but a large effort had to be spent in finding the optimum lip thickness, e , and the nozzle shape. The problem was complicated by the fact that preferred frequency of a free water-in-air jet is different from the submerged case. An ORGAN-PIPE system, if successful, would have the great advantage of very low losses.

Several techniques were used to determine the bunching characteristics of the SERVOJET and have all shown perfect correlations in the frequency spectra. Pressure oscillation measurements in the tube and on targets at various standoff distances showed the same characteristics as photographic observations and a laser beam interruption technique. This last technique looks the most promising; it has the advantage of giving, in real time with virtually no limitations, the bunching characteristics of the jet at any location downstream from the exit.

Several paint cleaning tests were performed and showed on aluminum panels a significant increase of the jet efficiency in the velocity region of maximum pressure oscillation intensity. These tests, as well as the optical and pressure measurement tests, showed the existence of an optimum standoff distance for maximum efficiency of the jet. This optimum standoff distance is that at which the jet just breaks up into slugs or droplets.

As expected and predicted by our analysis of bunching characteristics (Section III) this optimum standoff distance decreases with an increase of the relative pressure fluctuations and the Strouhal number. This explains the shift to lower standoff distances of the self excited jet when compared with the ordinary one. The range of the jet could be extended for the high pressure nozzles by choosing a lower Strouhal number and working at the optimum excitation levels which give, simultaneously, optimum range and cleaning rate. The cleaning rates in this case were as good as those obtained with a cavitating jet, with a standoff distance an order of magnitude higher.

The results of the analysis of bunching characteristic optimum frequencies for maximum cleaning rate, and the experimental results concerning the acoustical (internal pressure) properties of the jet will be very helpful for future development of this work. Such extension should include: a) an optimization of the PULSER-FED system for maximum cleaning rate; b) the increase of the working standoff distance by optimization of S_d and $p'/\Delta p$, as well as by reducing shear stresses and drag on the structured jet through air or water sheathing; c) a more precise experimental and theoretical study of the slug-coating interaction and, thus, a refinement of the criteria for an optimum jet oscillation frequency; d) development of the ORGAN-PIPE jet systems which would have less relative pressure oscillation, less losses and would,

HYDRONAUTICS, Incorporated

-43-

therefore, help to achieve our objectives of further increasing the jet "aggressivity" at increased standoff distances.

REFERENCES

1. Tierney, J. M., Doerschuk, D. C., and Abrams, H. C., "Mechanical Coating-Removal Techniques," AFML-TR-79-4174, Battelle Columbus Laboratory, December 1979. (The results in Table 2 of this report are from tests conducted at HYDRONAUTICS, Incorporated, February, 1979).
2. Gates, G., North Island Naval Air Station, Code 61225 NARF, private communications, April and August, 1981.
3. Lichtarowicz, A. and Nwachukwu, G., "Erosion by an Interrupted Jet," Proc. 4th International Symposium on Jet Cutting Technology, Cranfield, England, Paper B2, April 1978.
4. Summers, D. A., 1st Presentation, Session 3, Proceedings of the Workshop on the Application of High-Pressure Water Jet Technology, University of Missouri-Rolla, November 1975.
5. Erdmann-Jesnitzer, F., Louis, H. and Schikorr, W., "Cleaning, Drilling and Cutting by Interrupted Jets," Proc. 5th International Symposium on Jet Cutting Technology, Hanover, Federal Republic of Germany, Paper B1, June 1980.
6. Janakiram, K. S. and Syamala Rao, B. G., "Studies of the Characteristics of Flow and Erosion Due to Plain and CaviJet Impingement," Proc. 5th International Conference on Erosion by Solid and Liquid Impact, Cambridge, England, September 1979.
7. Cooley, W. C., "Rock Breakage by Pulsed High-Pressure Water Jets," Proc. 1st International Symposium on Jet Cutting Technology, Coventry, England, Paper B7, April 1972.
8. Nebeker, E. B. and Rodriguez, S. E., "Percussive Water Jets for Rapid Excavation," and "Development of Percussive Water Jets," Scientific Associates Technical Reports, 1973, and May 1979.
9. Conn, A. F., Johnson, V. E., Liu, H. L., and Frederick, G. S., "Evaluation of CAVIJET Cavitating Jets for Deep-Hole Rock Cutting," HYDRONAUTICS, Incorporated Technical Report 7821-1, August 1979.
10. Johnson, V. E., Jr., Chahine, G. L., Lindenmuth, W. T., Conn, A. F., Frederick, G. S., and Giacchino, G. J., Jr., "Cavitating and Structured Jets for Mechanical Bits to Increase Drilling Rate," A.S.M.E. paper, 82-Pet-13, 1982.

11. Johnson, V. E., Jr., Conn, A. F., Lindenmuth, W. T., Chahine, G. L., and Frederick, G. S., "Self-Resonating Cavitating Jets," Proceedings 6th International Symposium on Jet Cutting Technology, Surrey, England, April 1982.
12. Crow, S. C. and Champagne, F. H. "Orderly Structure in Jet Turbulence," Journal of Fluid Mechanics, Vol. 48, Part 3, pp. 547-591, August 1971.
13. Moore, C. J., "The Role of Shear Layer Instability Waves in Jet Exhaust Noise," Journal of Fluid Mechanics, Vol. 80, pp. 321-367, 1977.
14. Kibens, V., "Discrete Noise Spectrum Generated by an Acoustically Excited Jet," Paper 79-0592, AIAA Fifth Aeroacoustics Conference, March 12-14, 1979.
15. Morel, T., "Experimental Study of a Jet Driven Helmholtz Oscillator," ASME, Journal of Fluids Engineering, Vol. 191, pp. 383-390, September 1979.
16. Wylie, E. B., "Pipeline Dynamics and the Pulsed Jet," Proc., First Int'l Sympos. on Jet Cutting Technology (Coventry, U.K., April 5-7, 1972) Cranfield, U.K., BHRA Fluid Engineering, Paper A1, 12 pp., 1972.
17. Johnson, V. E., Jr., Lindenmuth, W. T., Conn, A. F., and Frederick, G. S., "Feasibility Study of Tuned-Resonator, Pulsing Cavitating Water Jet for Deep-Hole Drilling," HYDRONAUTICS, Incorporated Technical Report 8001-1, August 1980.
18. Sami, S. and Ansari, A., "Governing Equations in a Modulated Liquid Jet," Proc. 1st U.S. Water Jet Symposium, Golden, Colorado, Paper I.2, April 1981.
19. Clift, R., Grace, J. R., and Weber, M. E., "Bubbles, Drops and Particles," Academic Press, 1978.
20. Anno, J. N., "The Mechanics of Liquid Jets," Lexington Books, Lexington, MA, 1977.
21. Hammitt, F. G., "Cavitation and Multiphase Flow Phenomena," McGraw Hill International Book Company, 1980.

22. Theobald, C., "The Effect of Nozzle Design on the Stability and Performance of Turbulent Water Jets," Fire Safety Journal, 4, pp. 1-13, 1981.
23. Kibens, V., "Noise Generated by Large Scale Structures in An Axisymmetric Jet," Bull. Am. Phys. Soc., Vol. 23, pp. 1015ff, 1978.
24. Yamamoto, K. and Arndt, R. E. A., "Peak Strouhal Frequency of Subsonic Jet Noise as a Function of Reynolds Number," AIAA Journal, Vol. 17, No. 5, pp. 529-531, 1979.

HYDRONAUTICS, Incorporated

TABLE 1
Results from Paint Removal Tests on Aluminum Panel V

Run No.	Nozzle Type	Nozzle Pressure, Δp , psi	Standoff Distance, X, in.	Removal Rate, \bar{A} , ft ² /hr		
				Grey Topcoat	Tan Topcoat	Silver Topcoat
VC2a	Leach & Walker, d = 0.084 in.	5,080	9	28.1	12.5	1.9
VC1a			5	18.8	8.6	0.7
VC3a			13.5	31.3	12.5	3.9
VD1a			11 < X < 18	37.5	15.6	7.8
VD1a			18 < X < 23	37.5	12.5	6.3
VE1a	PULSER-FED SERVOJET, d = 0.10 in.	5,400	11 - 13.3	43.8	15.6	15.3
VB7a			11	31.3	14.1	14.1
VB6a			12.5 < X < 14.5	31.3	16.4	16.4
VB8a			11 < X < 13.5	40.6	14.8	14.8
VB1a			2	28.1	7	2.5
VB2a			4	-	8.6	7.4
VB3a			6	-	9.4	7.7
VB4a			7	-	10.9	8.6
VB5a	8 - 9	-	13.3	10.2		
VA4a	Leach & Walker (LW)	5,130	10	5.6	3.5	1.1
VA3a			4.8	9.4	6.6	4.7
VA2a	PULSER-FED (LW)	5,400	4.8	12.5	7.4	0.9
VA1a	PULSER-FED SERVOJET	5,400	4.8	28.1	9.4	6.3

HYDRONAUTICS, Incorporated

TABLE 2

Results from Paint Removal Tests on Aluminum Panel VII
Standoff distance: X = 13.5 in.

Run No.	Nozzle Type	Nozzle Pressure, Δp , psi	Removal Rate, \bar{A} , ft ² /hr		
			Grey Topcoat	Tan Topcoat	Yellow Primer
VIIA1a	PULSER-FED SERVOJET	4,950	25.0	14.1	10.8
VIIA2a	d = 0.10 in.	6,300	31.3	18	16.2
VIIA4a	Leach & Walker,	5,170	31.3	14.1	2.1
VIIA3a	d = 0.084 in.	6,580	25.0	15.6	7.0

HYDRONAUTICS, Incorporated

TABLE 3
Results from Paint Removal Tests on Aluminum Panel VI

Run No.	Nozzle Type*	Nozzle Pressure, Δp , psi	Standoff Distance, X, in.	Removal Rate, \bar{A} , ft ² /hr Grey Topcoat
V1D1a V1E1a	PF	5,400	3 10	0.3 0
V1E2a V1F1a	LW	5,080 5,920	10 13.5	7.1 6.6
V1F2a	PF	5,080	13.5	8.1
V1A6a V1A7a V1A8a	LW	5,080	11 13.5 11 to 23	2.6 3.8 3.0
V1B1a V1B2a V1B3a V1C1a	PF	5,400	5 9 13.5 11 to 15.5	0.4 0.4 1.9 0.3
V1A1a V1A2a V1A3a V1A4a V1A5a	LW	5,080	2 4 5 7 9	0.3 1.4 2.8 4.3 6.3

* PF: PULSER-FED SERVOJET, $d = 0.10$ in.; LW: Leach & Walker, $d = 0.084$ in.

HYDRONAUTICS, INCORPORATED

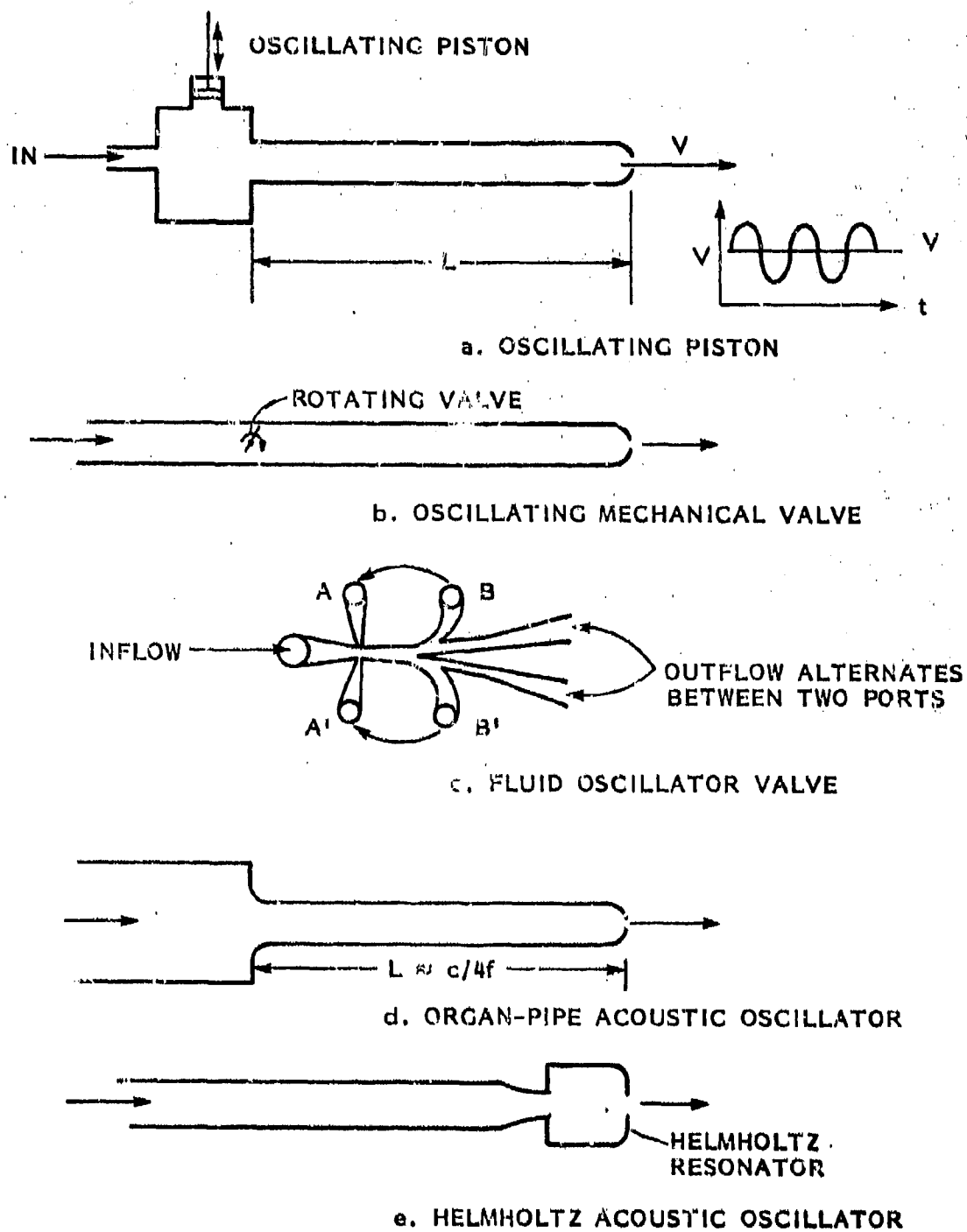
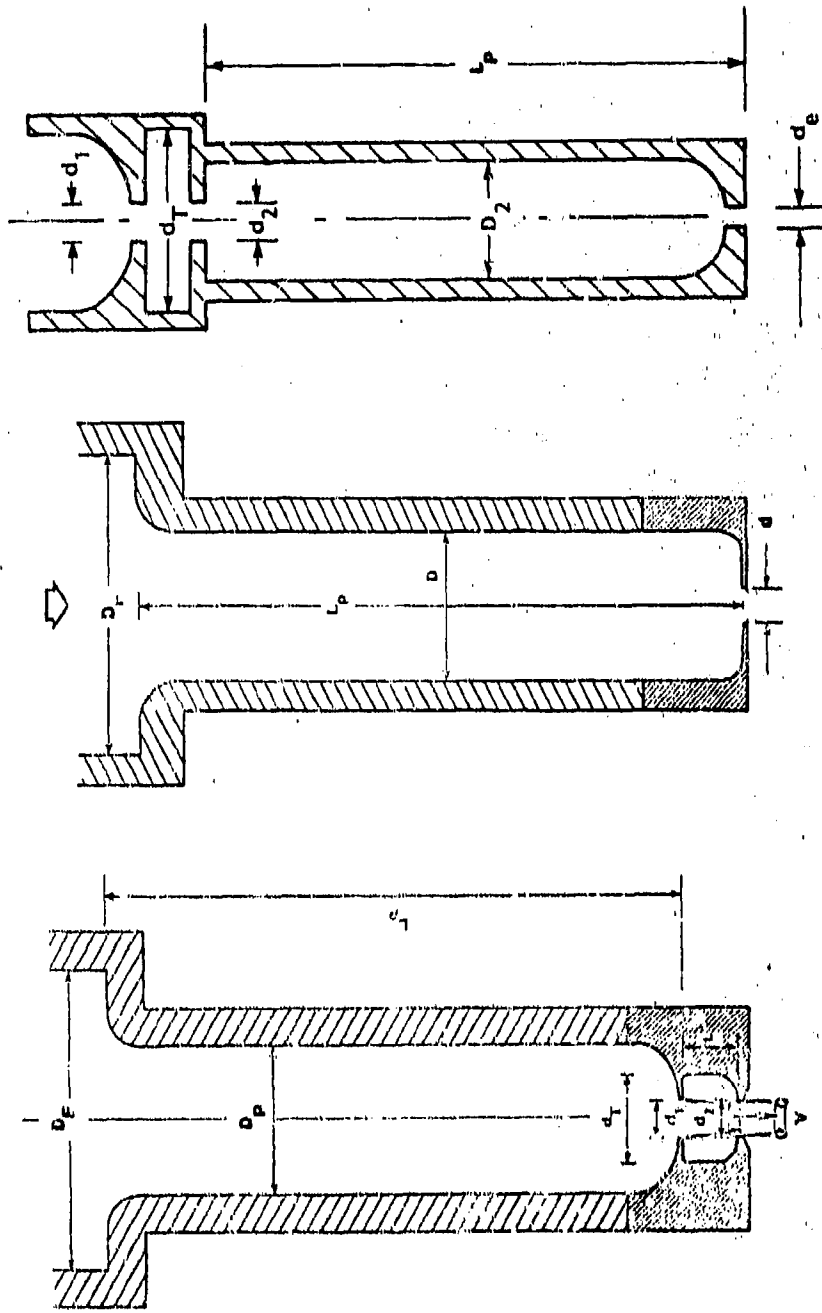


FIGURE 1 - GENERAL CONCEPTS FOR PULSING JETS



c. "PULSER-FED"

b. ORGAN-PIPE

a. "PULSER"

FIGURE 2 - SELF OSCILLATING NOZZLES: SERVOJET

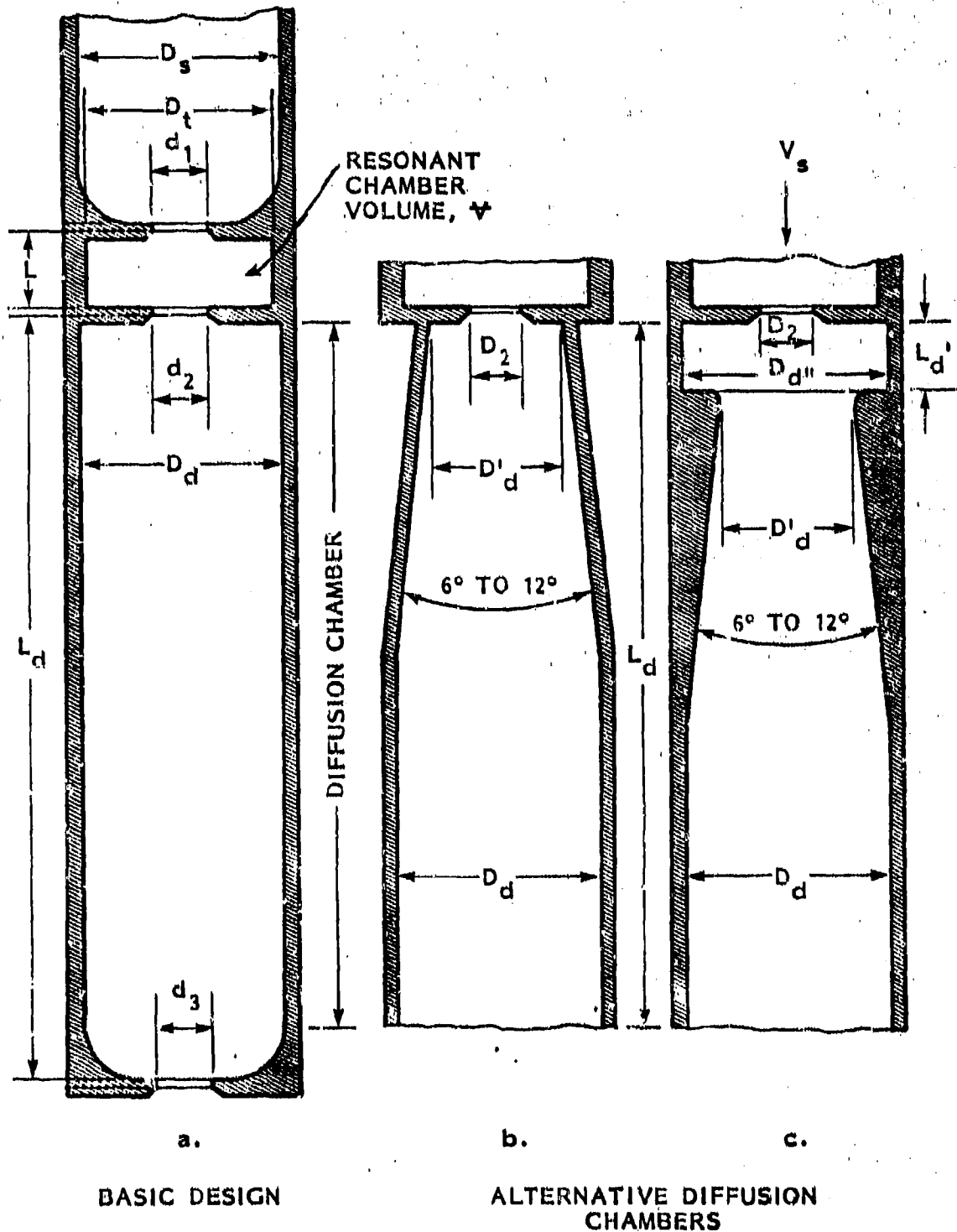
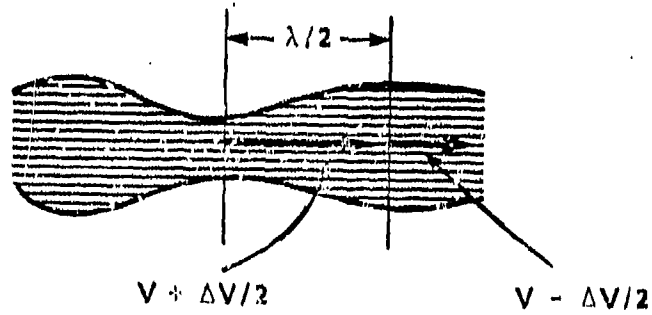
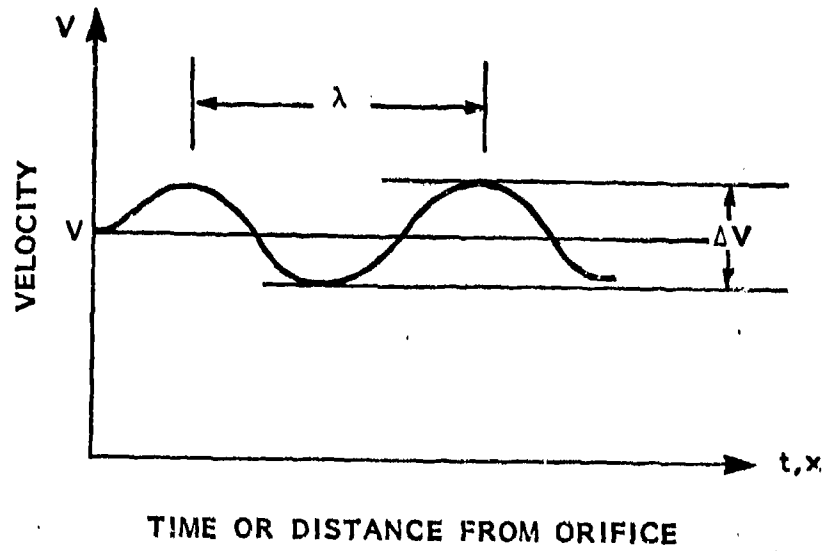


FIGURE 3 - CONCEPTS FOR PULSER-FED CAVIJET[®] NOZZLES

HYDRONAUTICS, INCORPORATED



TIME NEEDED FOR COMPLETE BUNCHING

$$T = \frac{\lambda}{2} / \Delta V$$

REQUIRED DISTANCE

$$X = TV = \frac{\lambda}{2} \cdot \frac{V}{\Delta V}$$

FIGURE 4 - RELATIONS FOR COMPLETE BUNCHING

HYDRONAUTICS, INCORPORATED

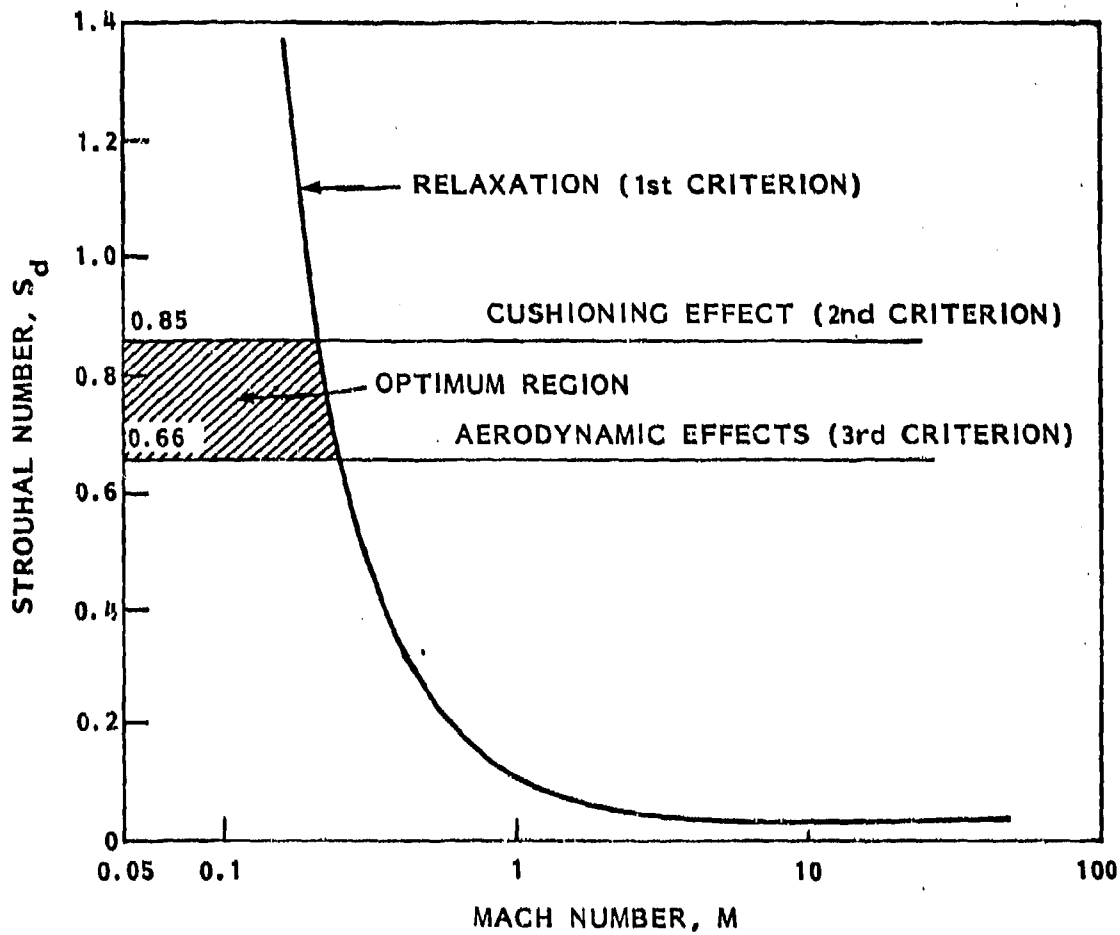


FIGURE 5 - CRITERIA FOR OPTIMIZING THE FREQUENCY OF PULSED JETS

HYDRONAUTICS, INCORPORATED

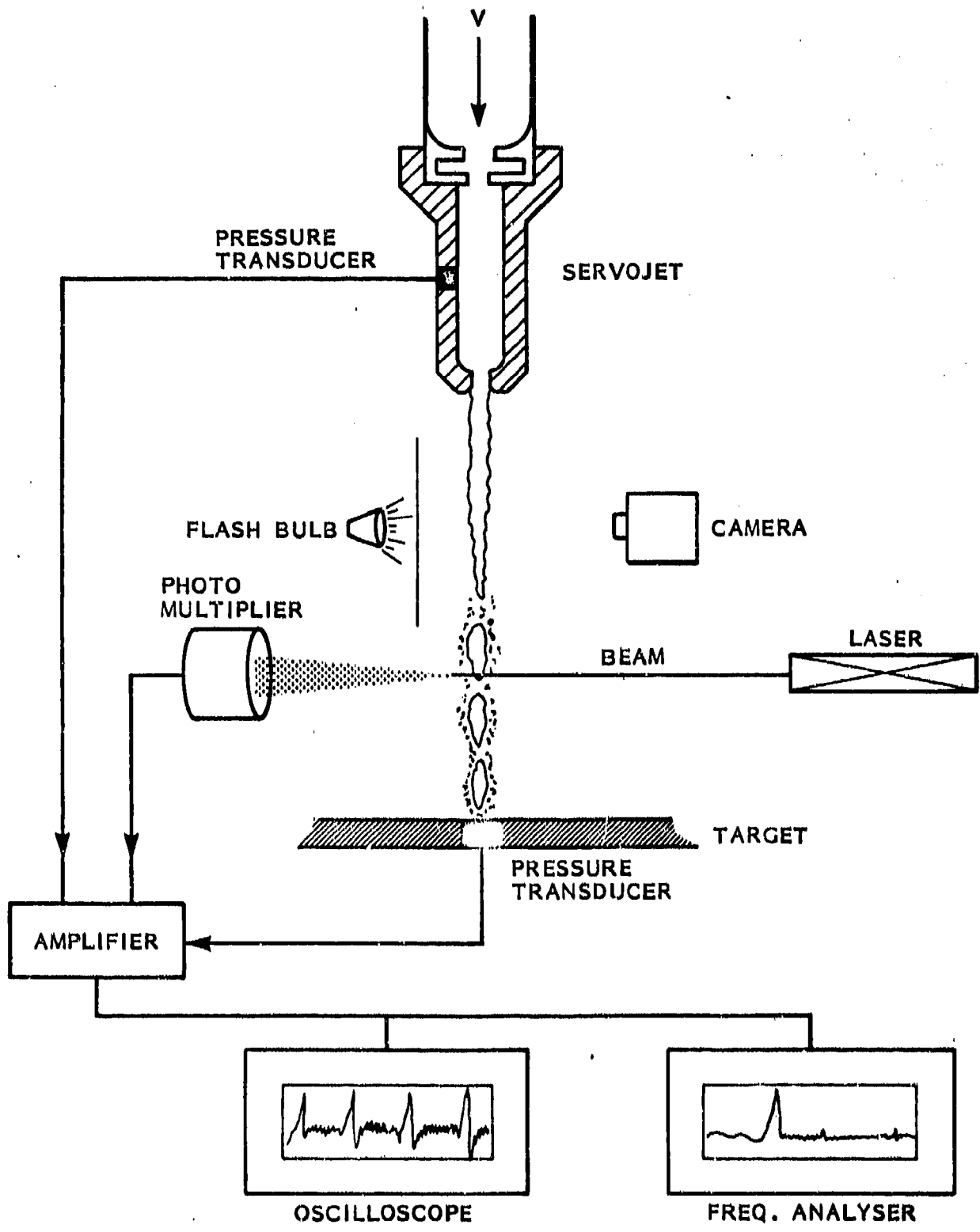
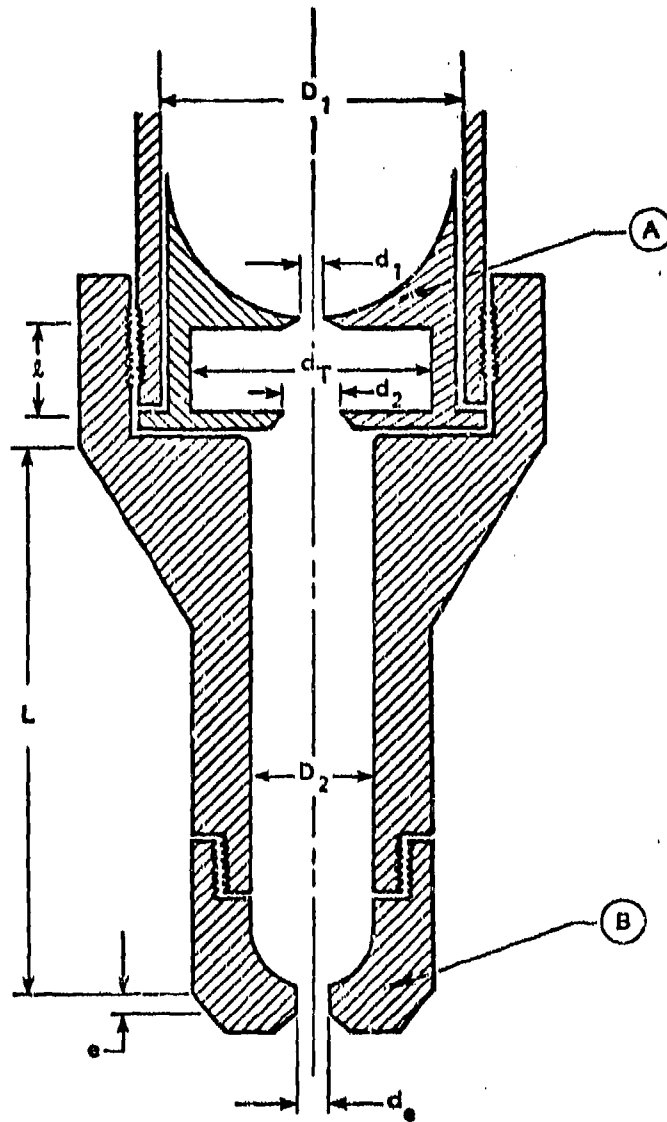


FIGURE 6 - EXPERIMENTAL SETUP



PULSER-FED AND ORGAN-PIPE

FIGURE 7 - SCHEMATIC OF SERVOJET NOZZLES CONSTRUCTED

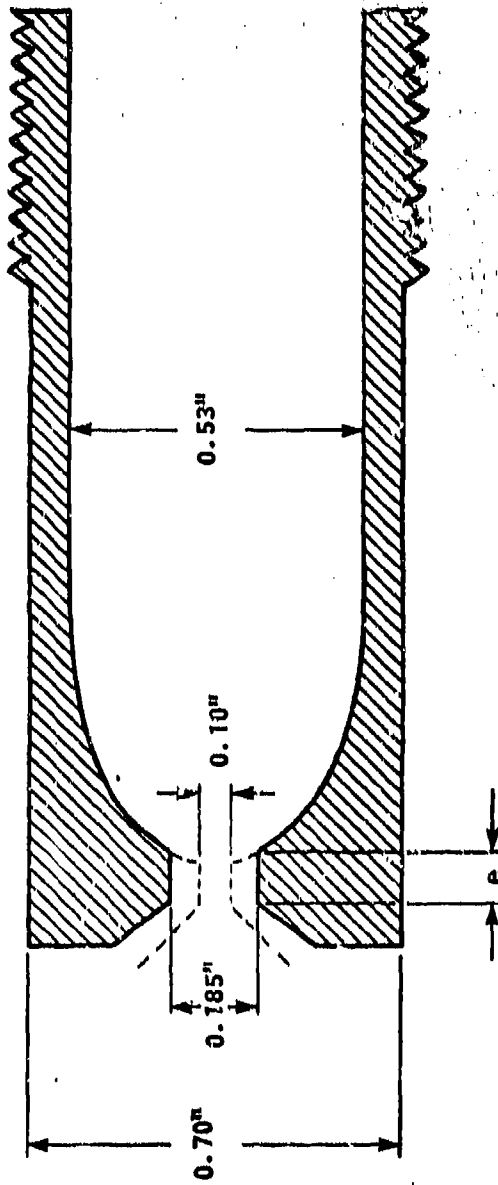


FIGURE 8 - CAVIJET[®] ELLIPTICAL SHAPE USED

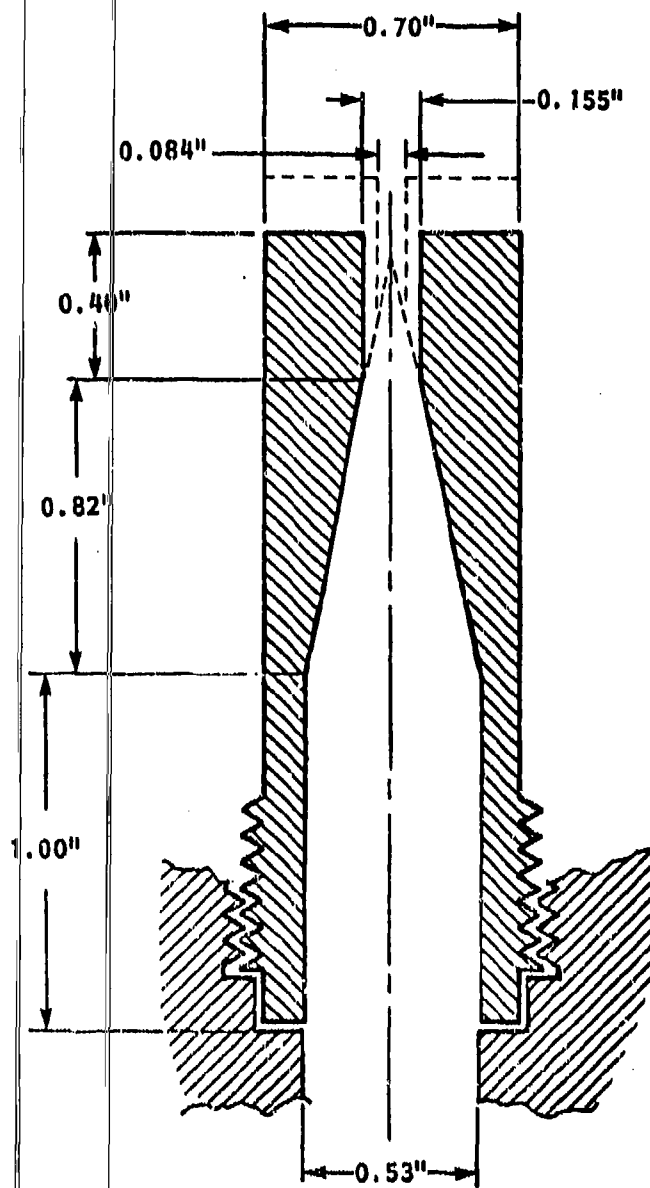


FIGURE 9 - LEACH AND WALKER NOZZLE USED

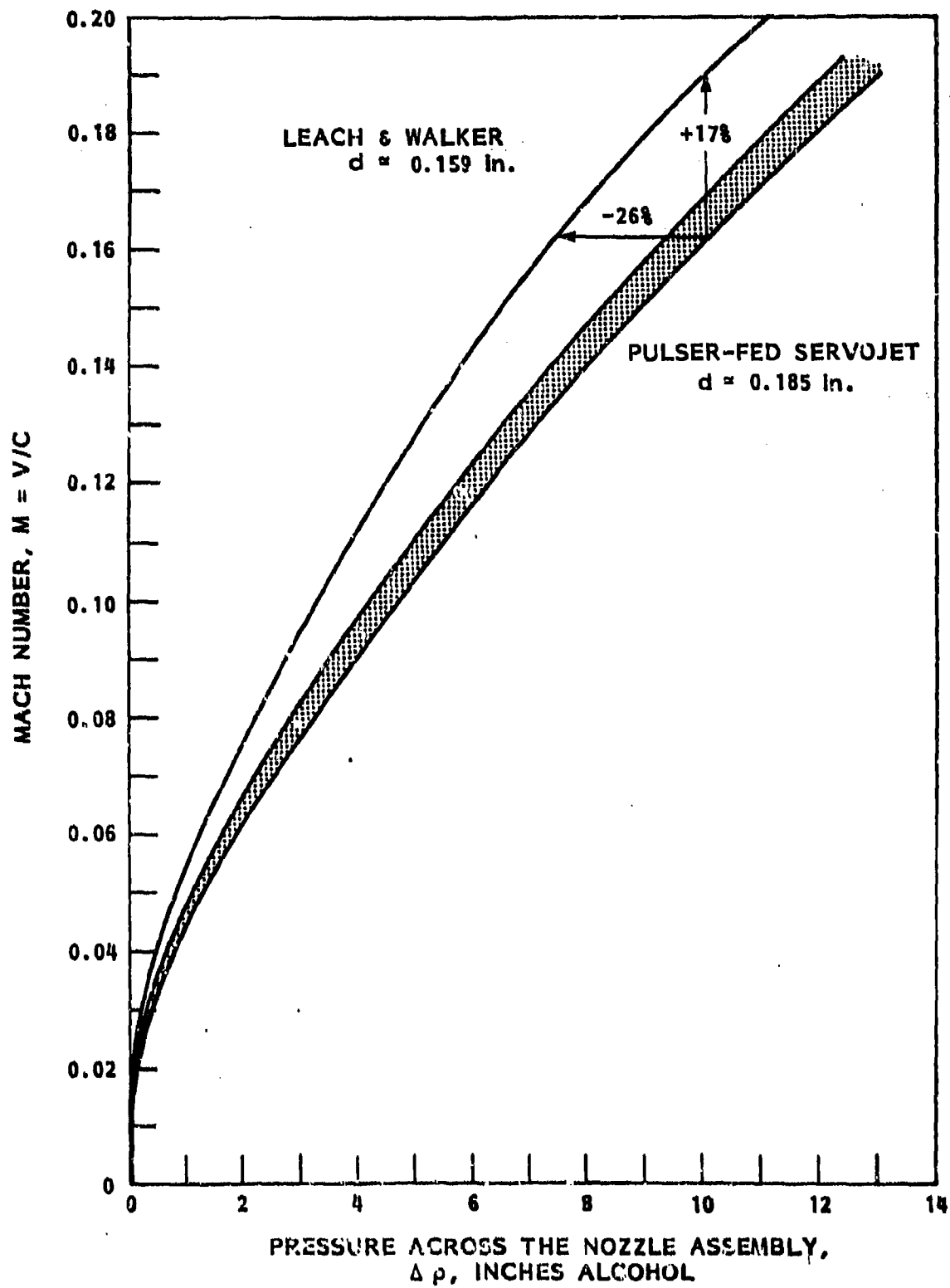


FIGURE 10 - DISCHARGE CURVES FOR THE NOZZLES USED

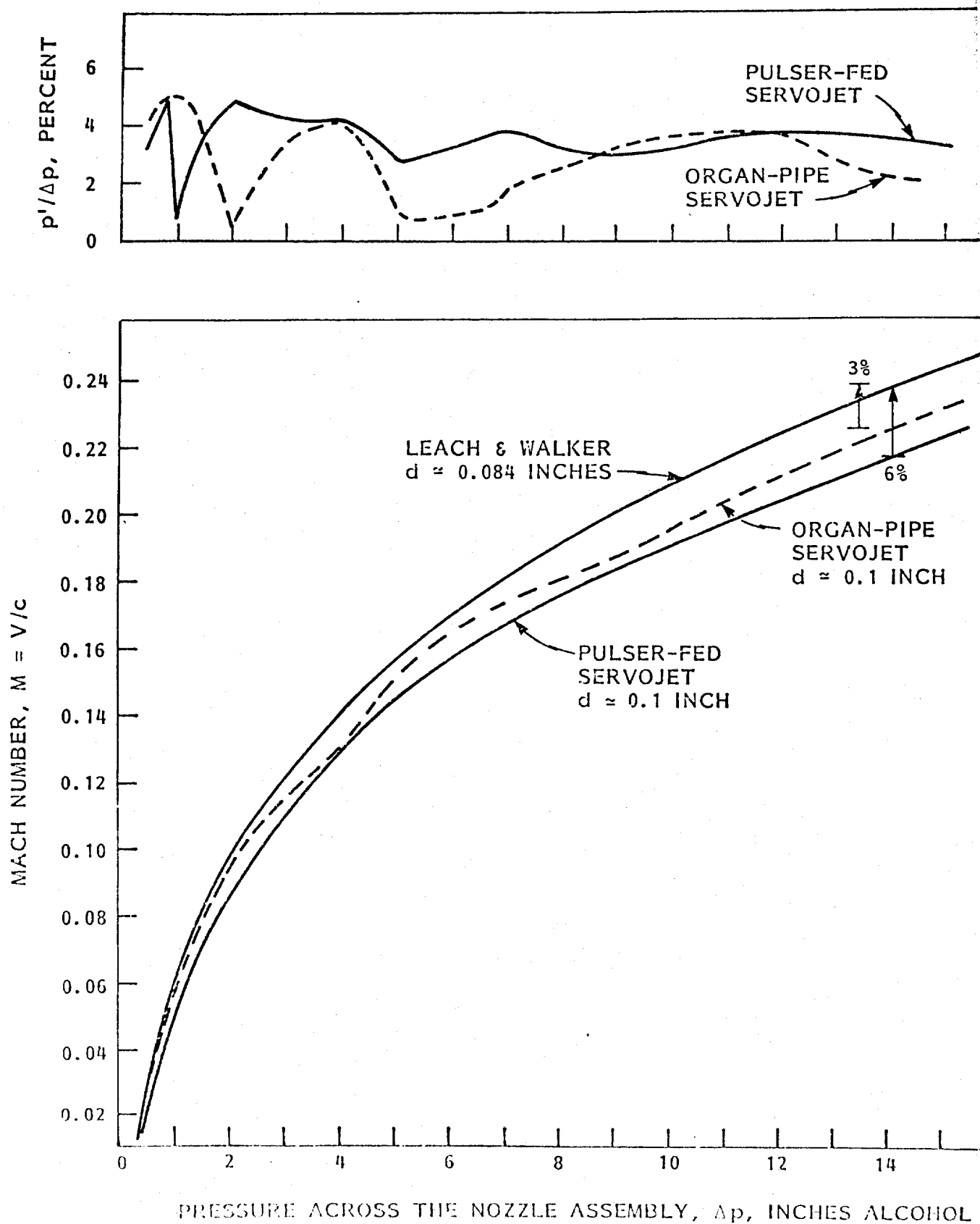


FIGURE 11 DISCHARGE CURVES AND PRESSURE OSCILLATIONS FOR THE NOZZLES USED

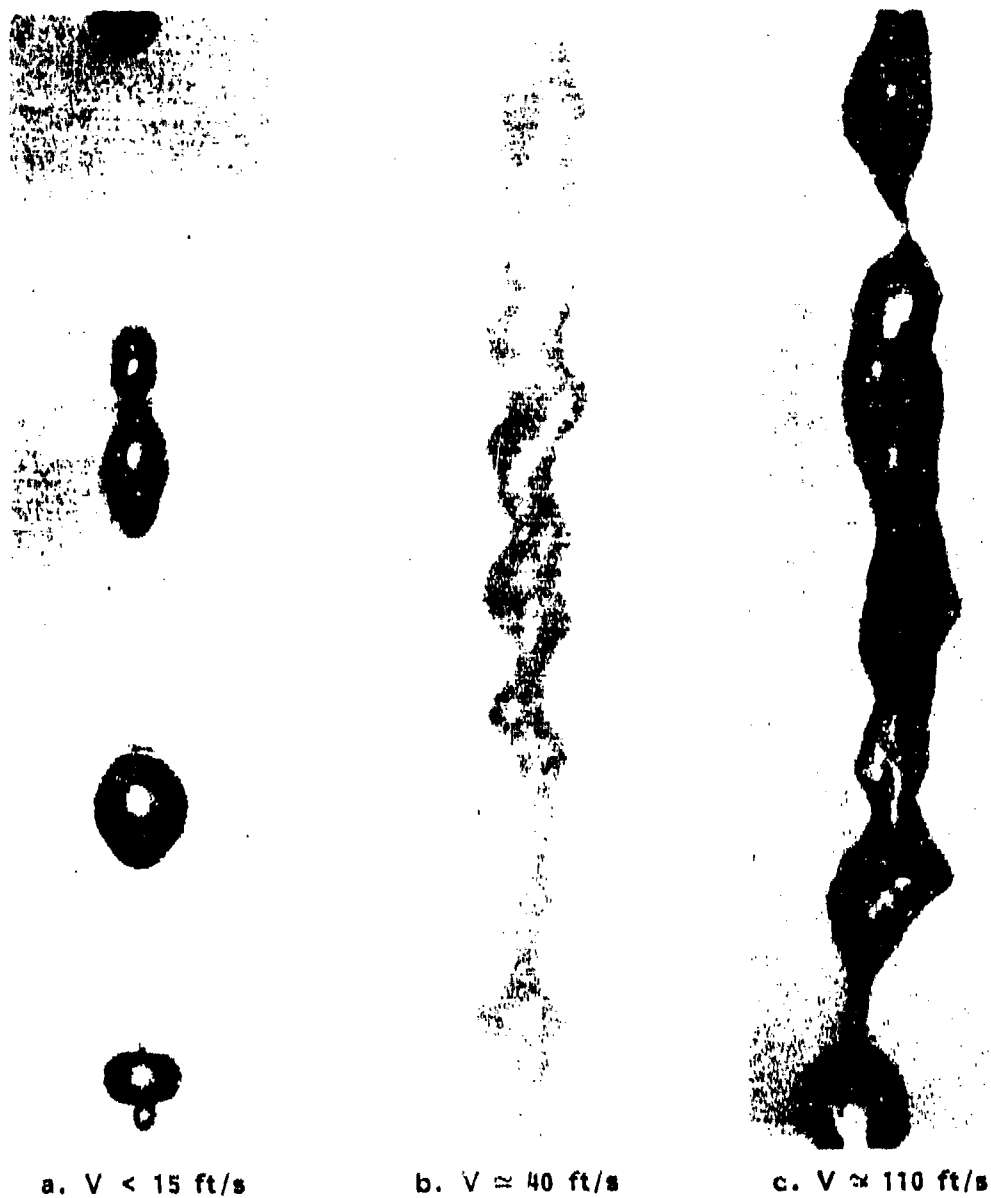


FIGURE 12 - OSCILLATION AND PRODUCTION OF DROPS IN RELATIVELY LOW VELOCITY JETS

HYDRONAUTICS, INCORPORATED

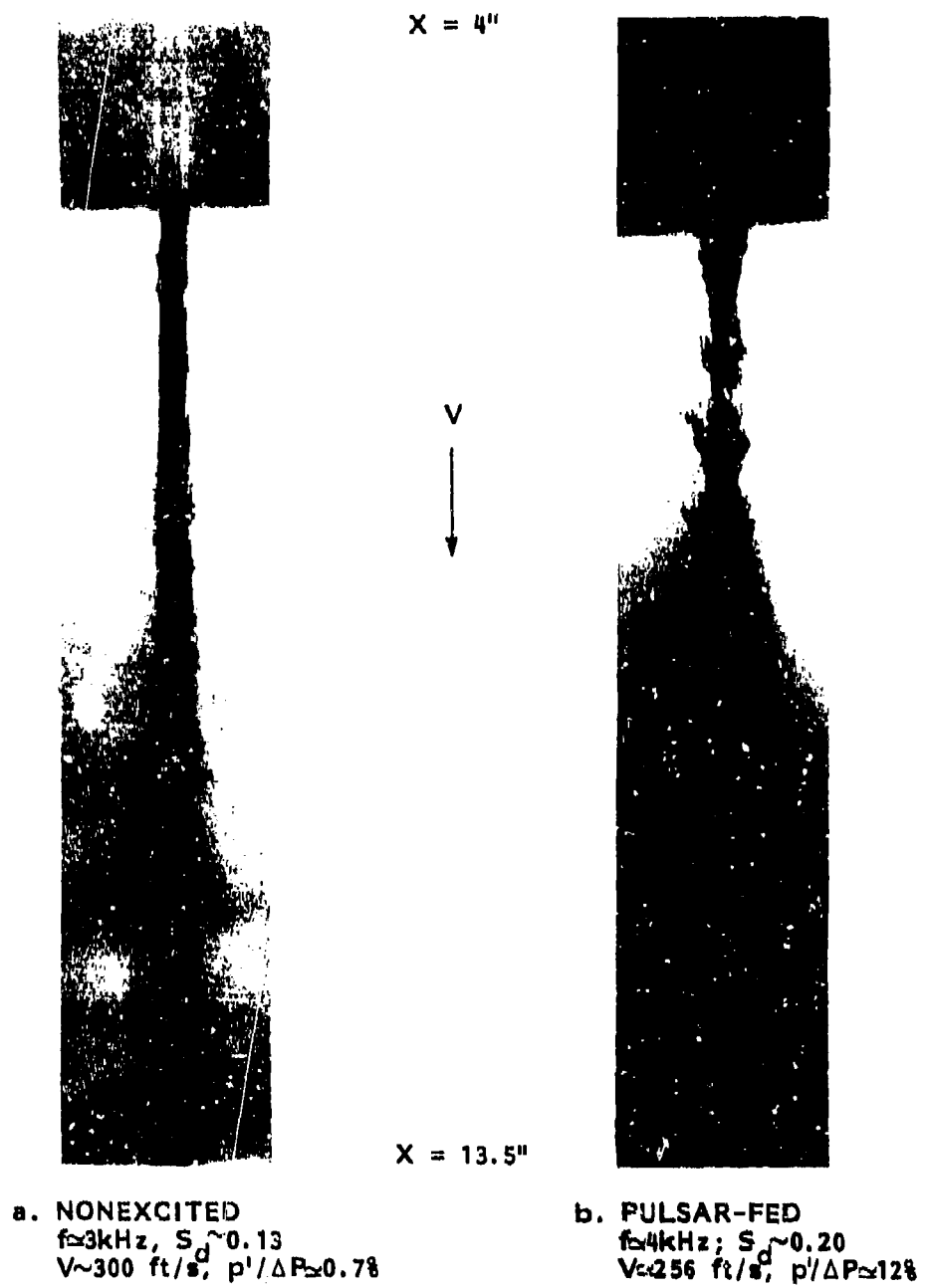
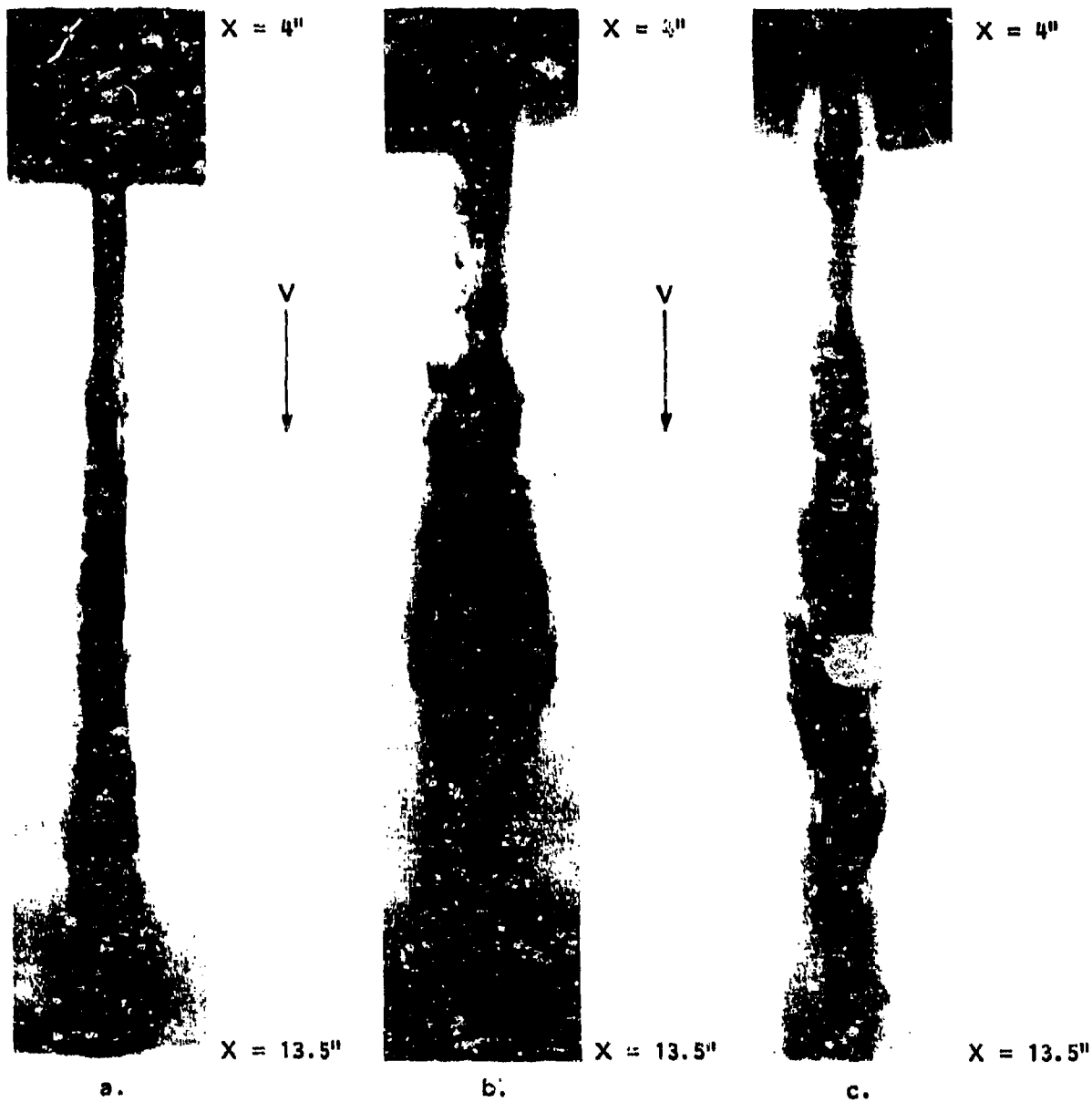


FIGURE 13 - JET APPEARANCE AT A TOTAL PRESSURE DROP ACROSS THE NOZZLE ASSEMBLY OF 800 psi FOR A LEACH & WALKER NOZZLE SHAPE, $d \approx 0.155\text{ INCH}$

HYDRONAUTICS, INCORPORATED



NONEXCITED
 $F \approx 3\text{kHz}$, $S_{cr} \approx 0.11$
 $V \approx 365\text{ ft/s}$, $p'/\Delta P \approx 0.68$

PULSAR FED
 $F \approx 3.8\text{kHz}$, $S_{cr} \approx 0.15$
 $V \approx 320\text{ ft/s}$, $p'/P \approx 5.98$

FIGURE 14 - JET APPEARANCE AT A TOTAL PRESSURE DROP ACROSS THE NOZZLE ASSEMBLY OF 920 psi FOR A LEACH & WALKER NOZZLE SHAPE, $d \approx 0.155\text{ INCH}$



FIGURE 15 - JET APPEARANCE IN THE MAXIMUM OSCILLATION REGION. PULSAR-FED, $d \sim 0.185$ INCHES, $e \sim 0.02$ INCHES

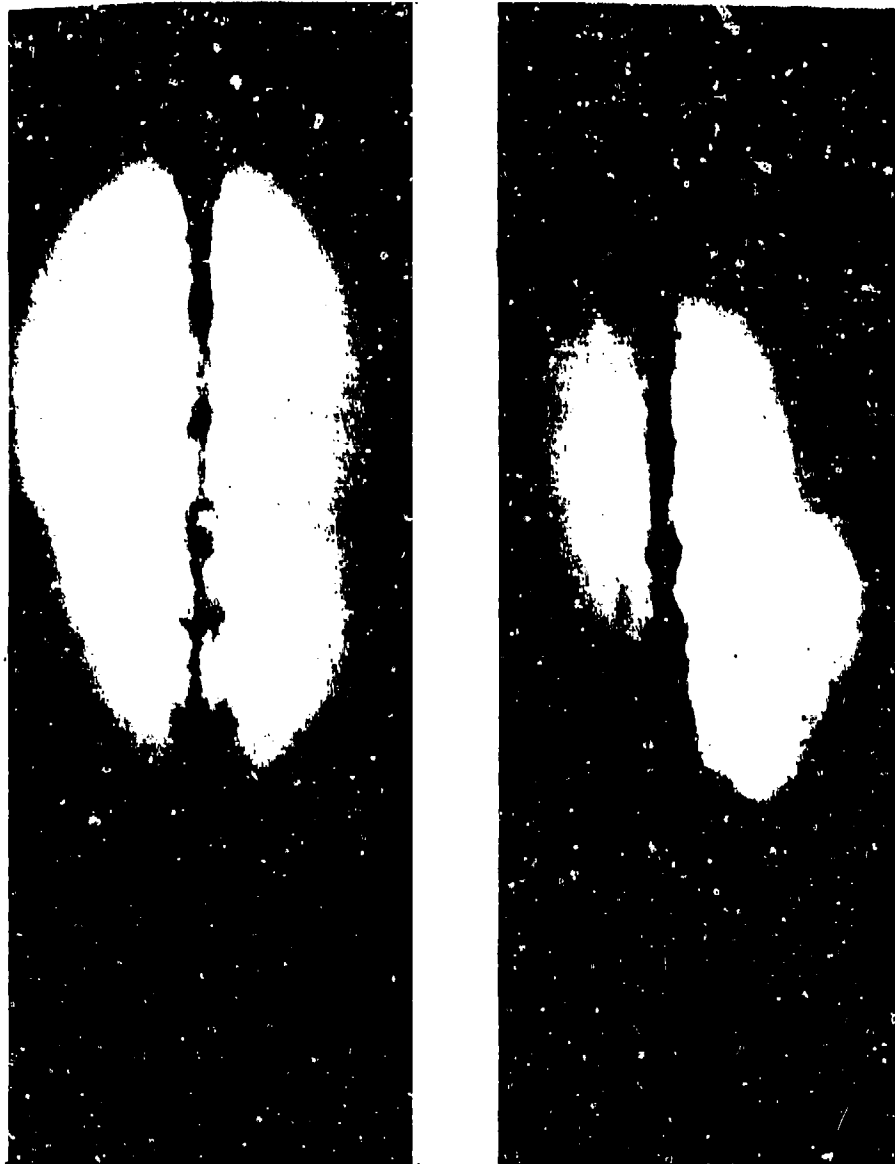


FIGURE 16 - JET APPEARANCE OF A PULSER-FED SERVOJET,
 $\Delta p \approx 810$ psi, $d \approx 0.10$ in., $f = 3.6$ kHz

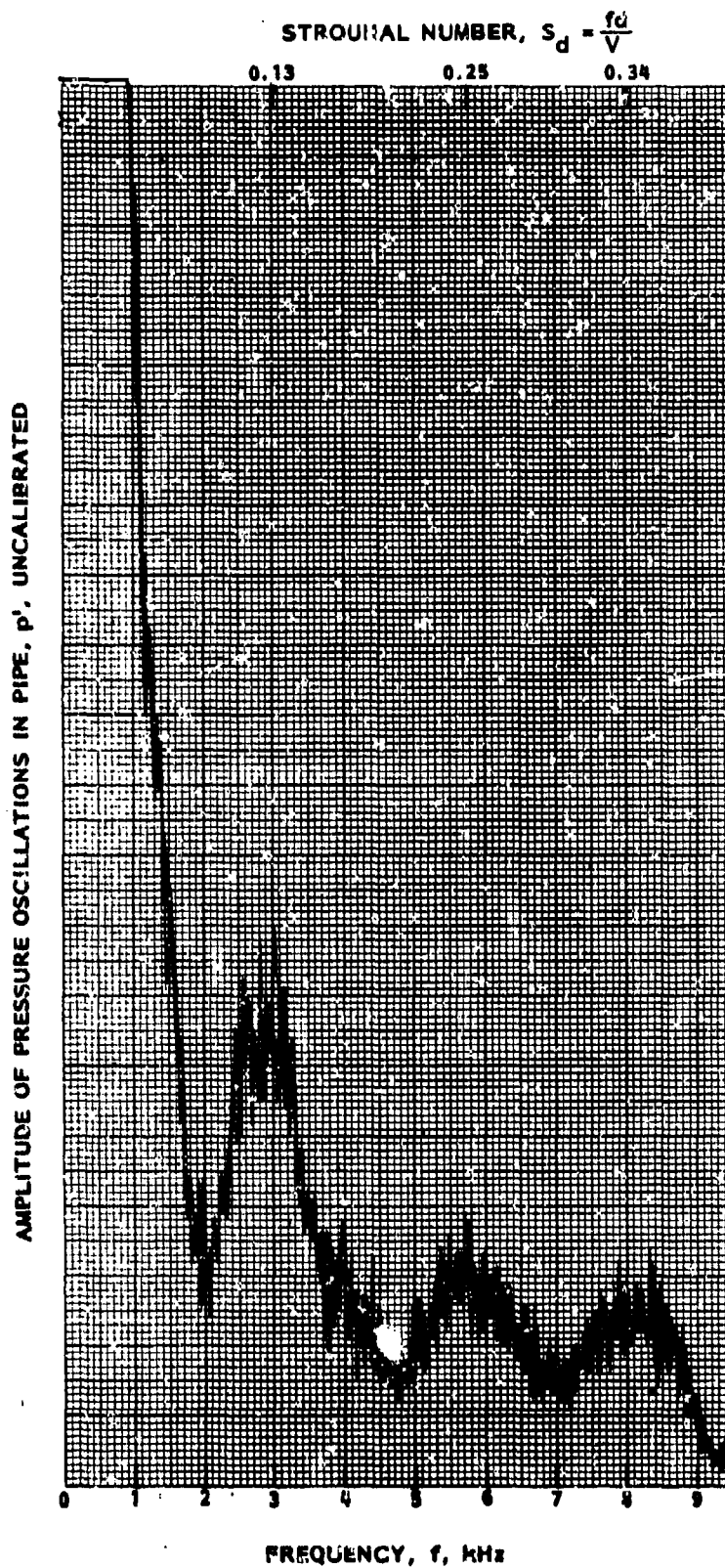


FIGURE 17 - FREQUENCY SPECTRUM FOR A CAVIJET[®] NONEXCITED
 JET, $d \approx 0.185$ inches, $a \approx 0.02$ inches, $V \approx 360$ ft/s,
 $p'/\Delta p \approx 0.48$

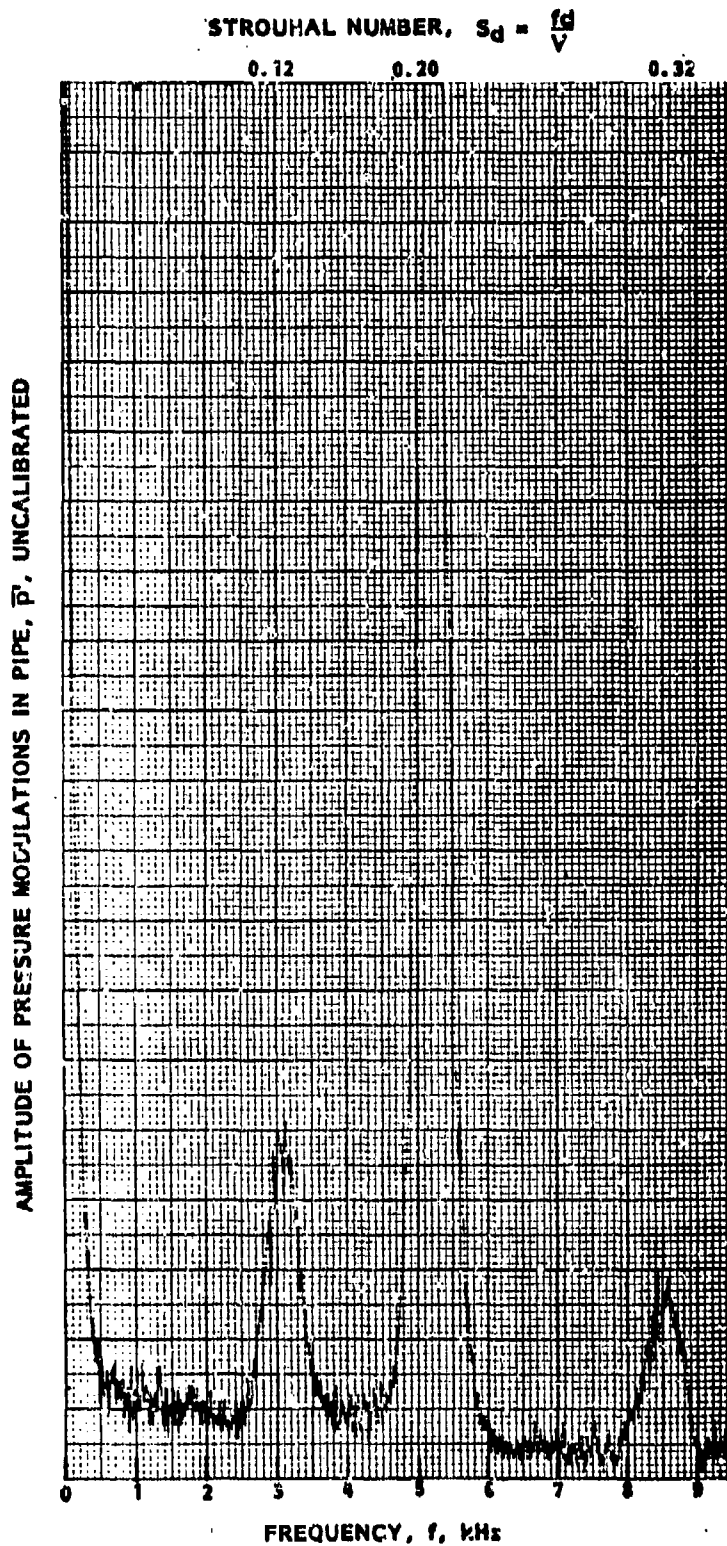


FIGURE 18 - FREQUENCY SPECTRUM FOR A PULSER-FED CAVIJET[®]
 NOZZLE, $d \approx 0.185$ inches, $e \approx 0.02$ inches, $V \approx 360$ ft/s.,
 $p'/\Delta p \approx 5.28$

HYDRONAUTICS, INCORPORATED

STROUHAL NUMBER, $S_d = \frac{fd}{V}$

0.20

0.33

AMPLITUDE OF PRESSURE OSCILLATIONS, p' , UNCALIBRATED

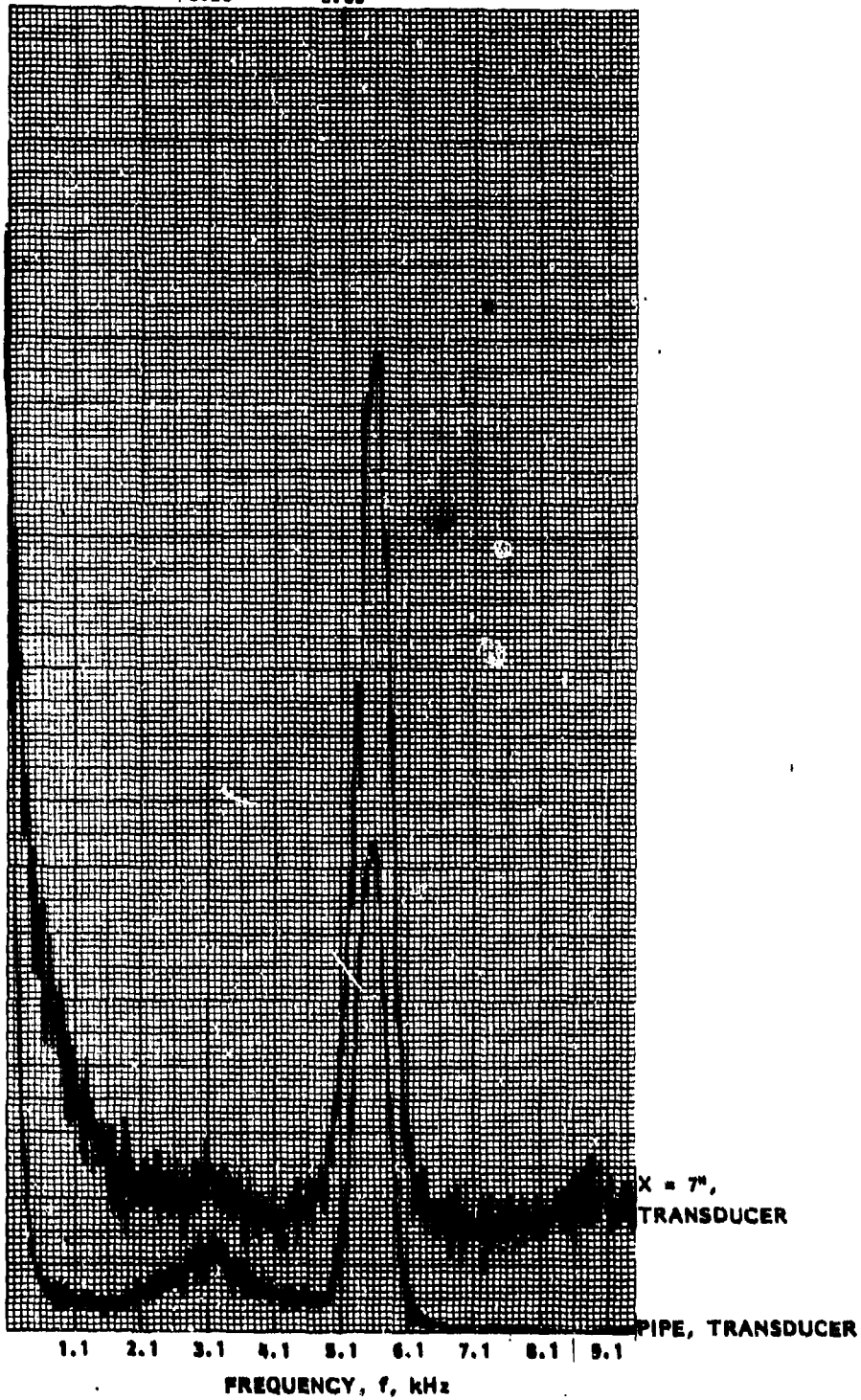


FIGURE 19 - COMPARISON BETWEEN FREQUENCY SPECTRA OF PRESSURE OSCILLATION IN PIPE AND ON TARGET AT OPTIMUM STANDOFF DISTANCE, $X \approx 7$ INCHES, $d \approx 0.185$ INCHES, $e \approx 0.02$ INCHES, $V \approx 210$ ft/s, $(p'/\Delta p)_{\text{pipe}} \approx 3.5\%$, $(p'/\Delta p)_{\text{target}} \approx 13.5\%$

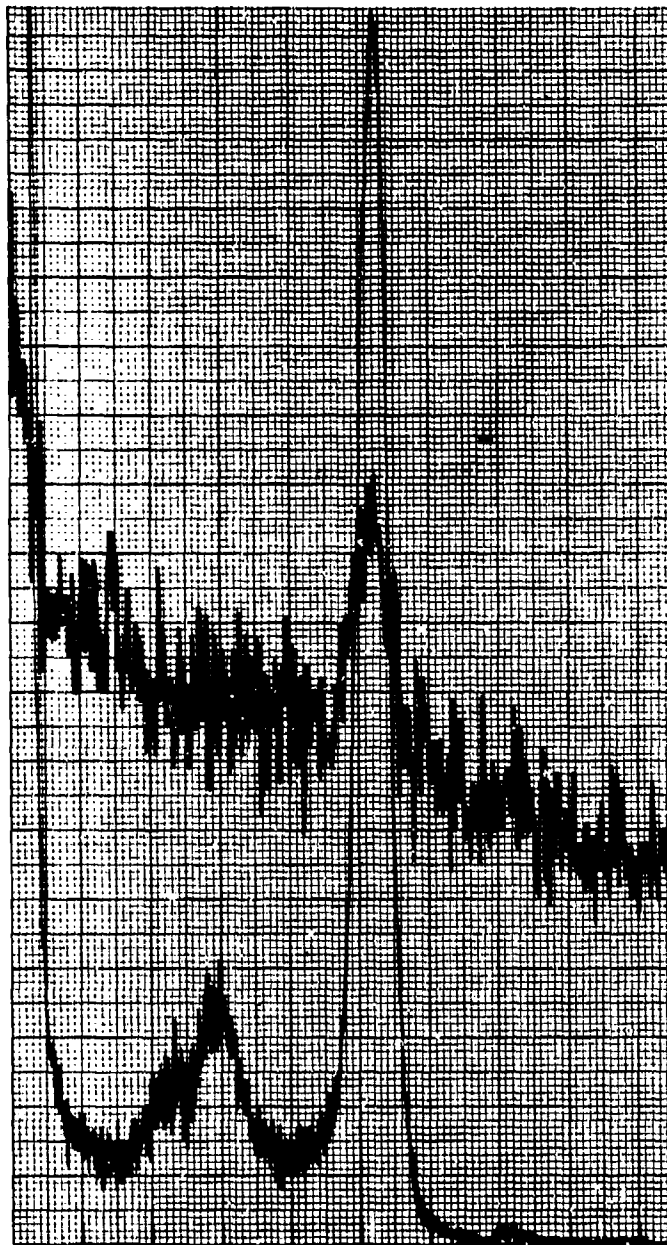
HYDRONAUTICS, INCORPORATED

$$\text{STROUHAL NUMBER, } S_d = \frac{fd}{V}$$

0.20

0.33

AMPLITUDE OF OSCILLATIONS



X = 10 INCHES, LASER

PIPE, TRANSDUCER

0.1 1.1 2.1 3.1 4.1 5.1 6.1 7.1 8.1

FREQUENCY, f, kHz

FIGURE 20 - COMPARISON BETWEEN PRESSURE OSCILLATIONS IN PIPE SPECTRUM AND LIGHT INTERRUPTION FLUCTUATIONS SPECTRUM, $d \approx 0.165$ INCHES, $V \approx 205$ ft/s, $p'/\Delta P \approx 8.38$

HYDRONAUTICS, INCORPORATED

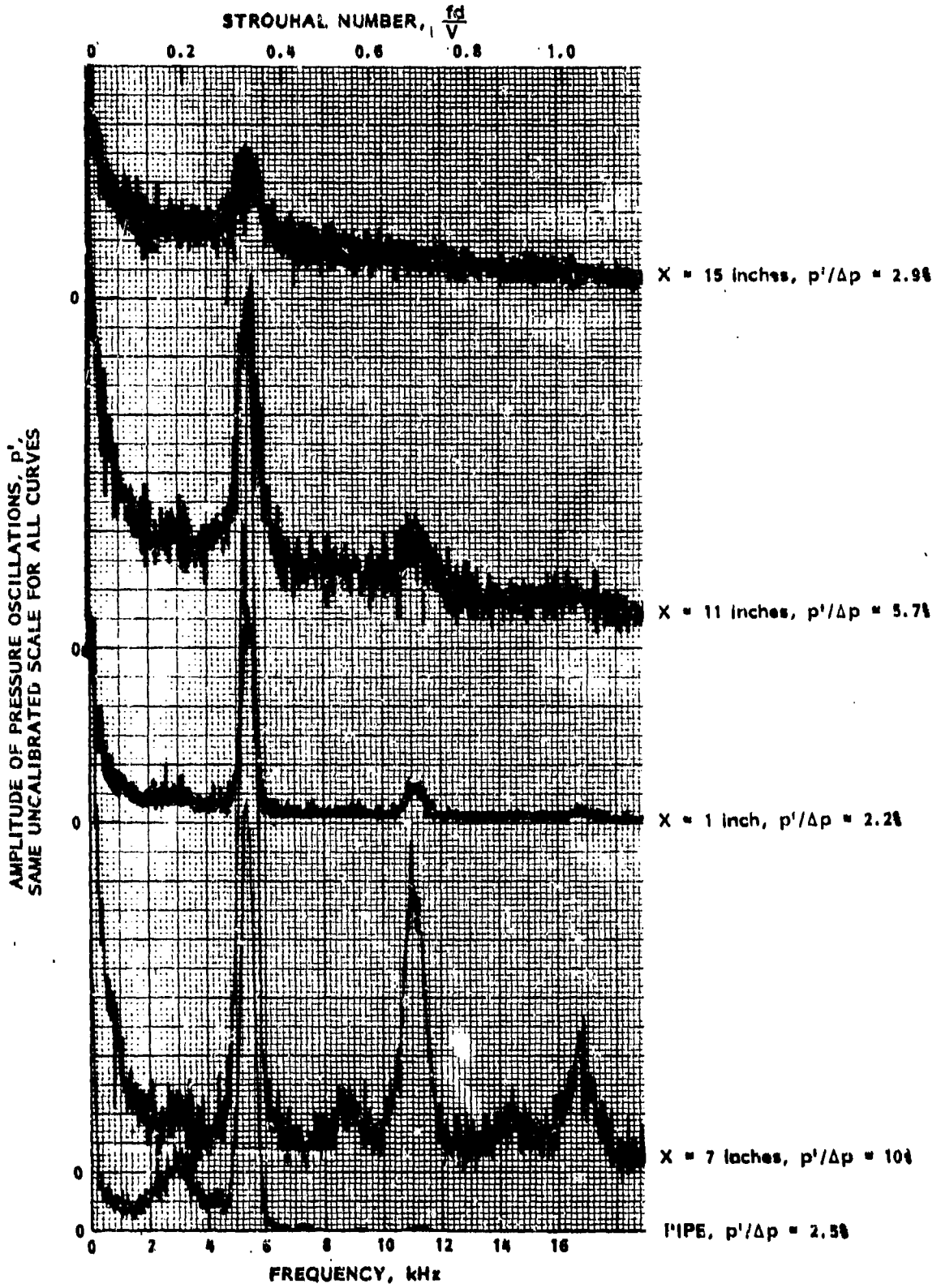


FIGURE 21 - PRESSURE FLUCTUATIONS IN PIPE AND ON TARGET
TRANSDUCER AT SEVERAL STANDOFF DISTANCES,
 $V \approx 215$ ft/s, $d \approx 0.185$ inches

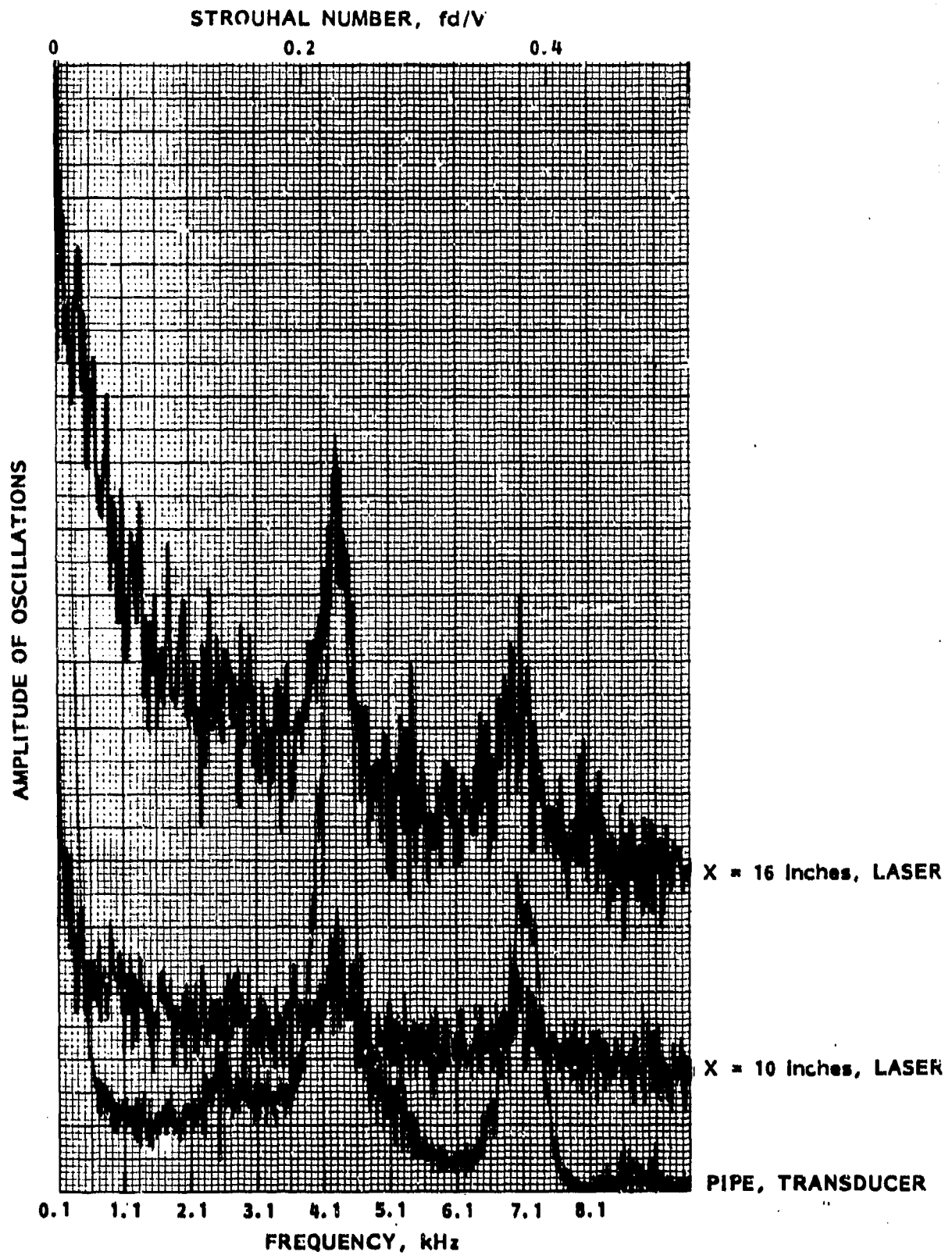


FIGURE 22 - COMPARISON BETWEEN PRESSURE OSCILLATIONS IN PIPE SPECTRUM AND LIGHT INTERRUPTION FLUCTUATIONS SPECTRA, $V \sim 296$ ft/s., $d \approx 0.185$ inches

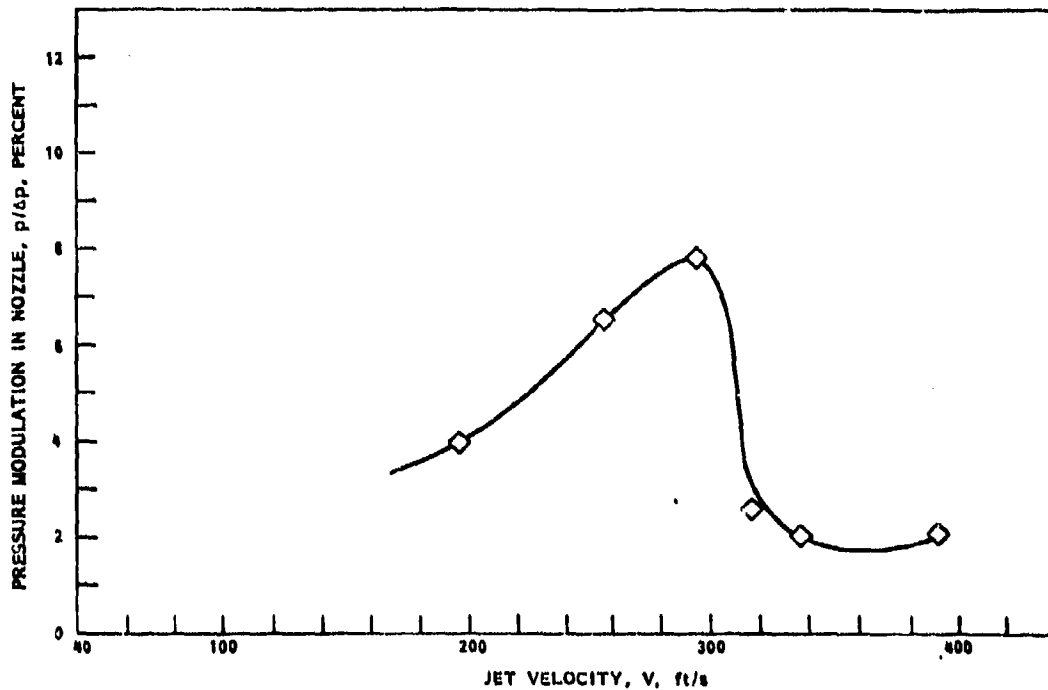
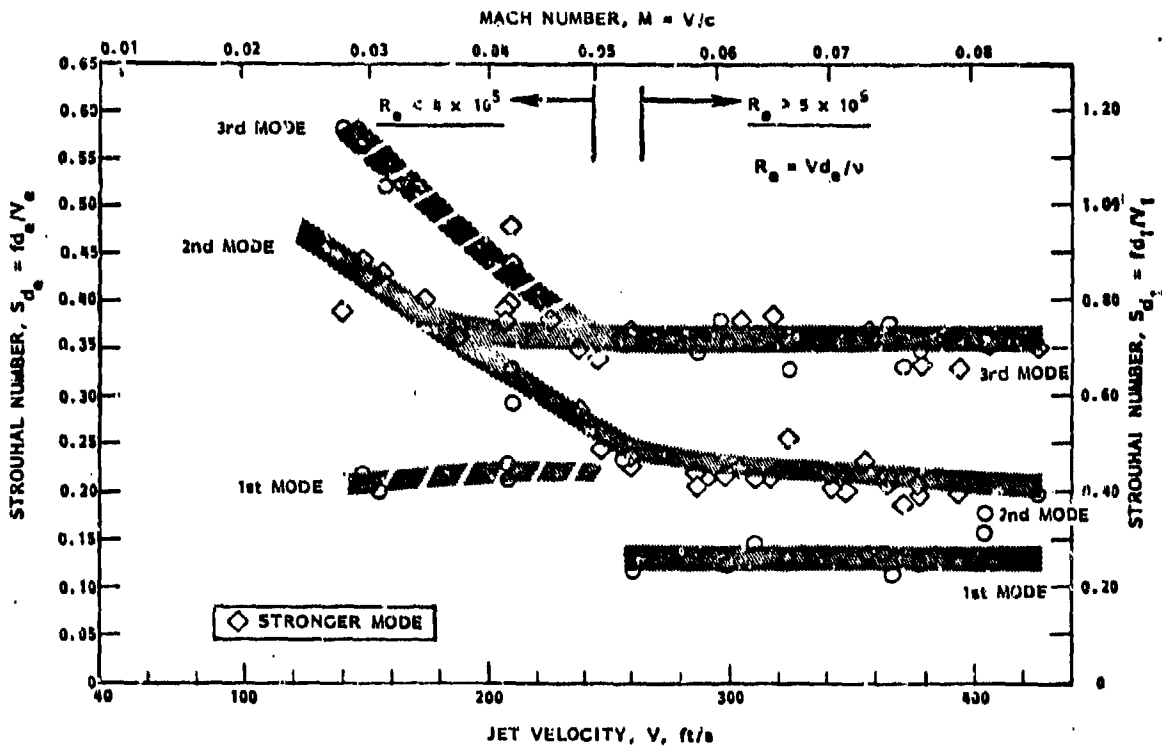


FIGURE 23 - ACOUSTICAL CHARACTERISTICS OF A PULSER-FED SERVOJET, $d = 0.185$ INCHES, $d_1 = 0.23$ INCHES
 $L = 0.37$ INCHES

HYDRONAUTICS, INCORPORATED

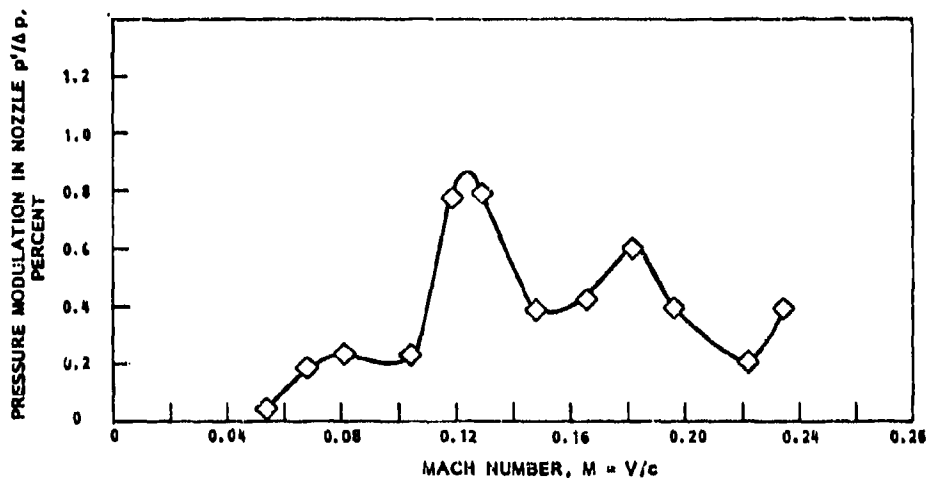
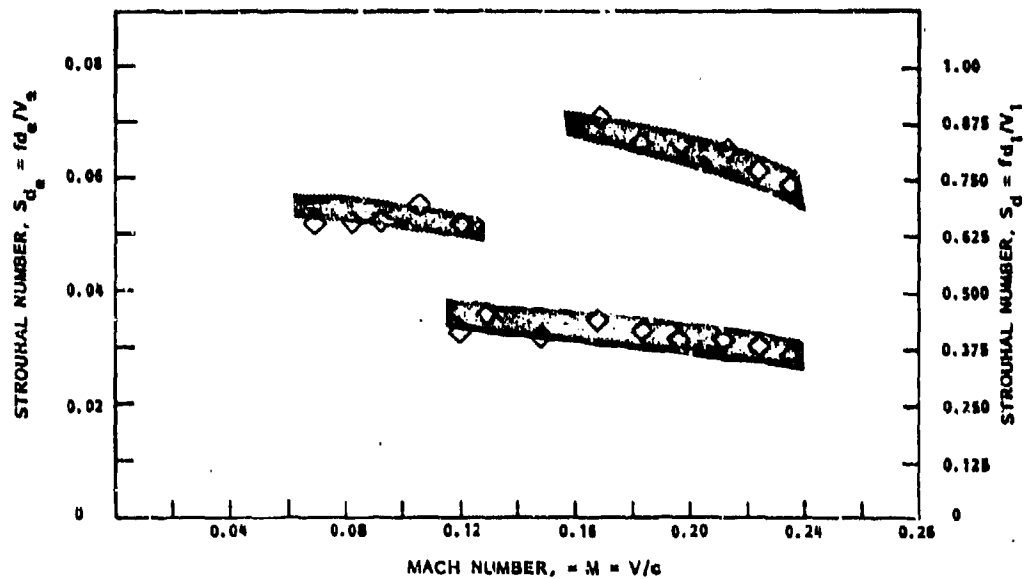


FIGURE 26 - ACOUSTICAL CHARACTERISTICS OF A PULSER FED SERVOJET, $d_0 = 0.10$ INCHES, $d_1 = 0.23$ INCHES, $l = 0.37$ INCHES

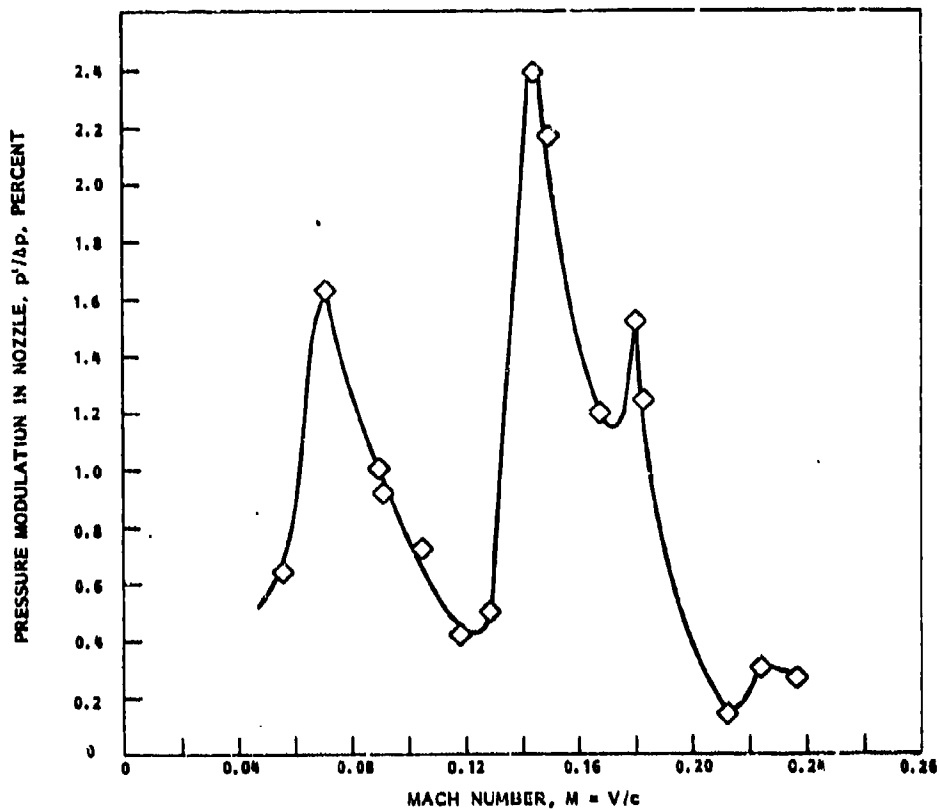
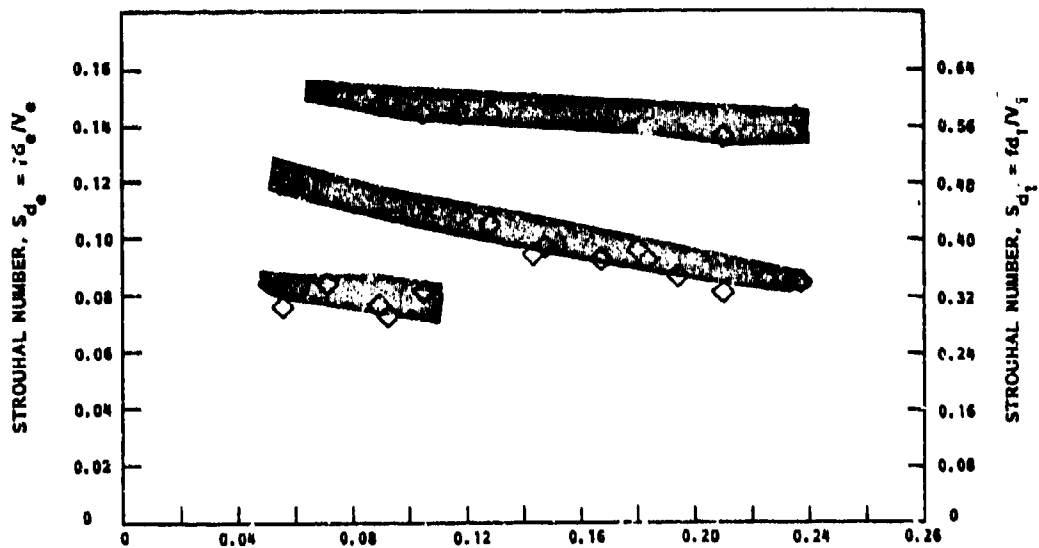


FIGURE 25 - ACOUSTICAL CHARACTERISTICS OF A PULSER-FED SERVOJET, $d_0 = 0.10$ INCHES, $d_1 = 0.159$ INCHES, $\lambda = 0.255$ INCHES

HYDRONAUTICS, INCORPORATED

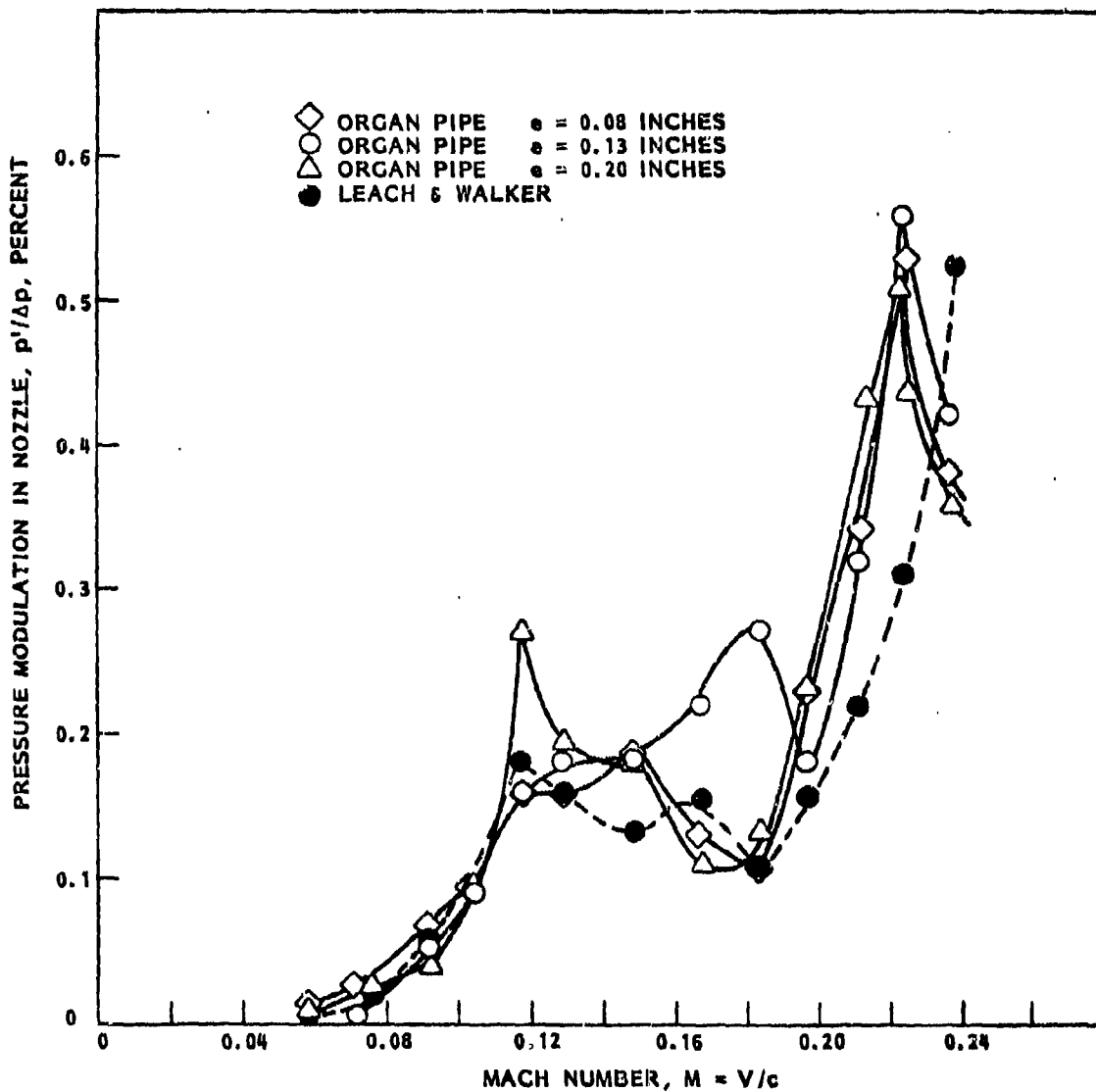
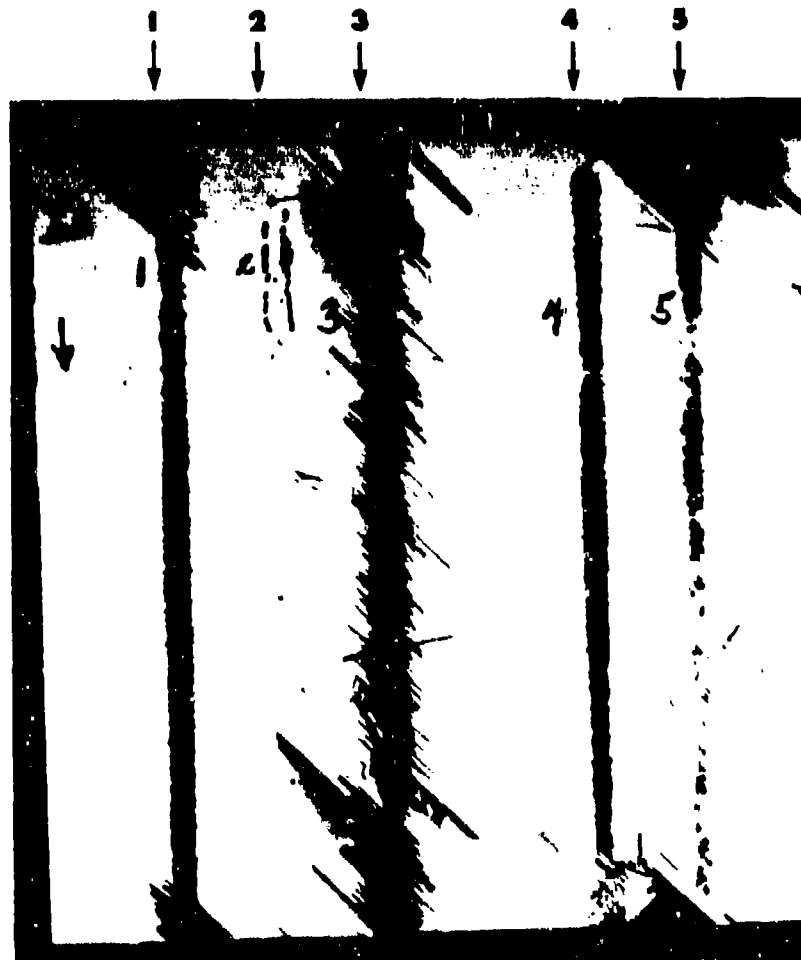


FIGURE 26 - PRESSURE OSCILLATIONS IN ORGAN-PIPE AND LEACH AND WALKER NOZZLES TESTED

HYDRONAUTICS, INCORPORATED



RUN	TRANSLATION VELOCITY, in./s	STANDOFF X, in.	NOZZLE PRESSURE, Δp , psi
1	1.0	4.0	5,220
2	1.0	4.0	3,420
3	1.5	4.0	5,220
4	1.5	4.0	5,220
5	1.5	4.5	5,100

FIGURE 27 - NONUNIFORM PAINT CLEANING IN REINFORCED CARBON-FIBER PANELS. PANEL IA, PULSER-FED SERVOJET



RUN	NOZZLE TYPE*	TRANSLATION VELOCITY, in./s	STANLOFF, X, in.	NOZZLE PRESSURE, P, psi
1	PF	1.0	4.75	5,220
2	PF	1.0	4.75	6,300
3	PF	1.0	4.75	7,380
4	OP	1.0	6 TO 24	6,300
4a	LW	1.0	10.25	5,220
5	PF	1.0	4.75	5,220
7	PF	1.0	4.75	6,300
8**	LW	1.0	19	7,380

*PF: PULSER-FED SERVOJET; OP: ORGAN-PIPE SERVOJET;
LW: LEACH & WALKER

**PANEL WAS CUT THROUGH DURING THIS RUN

FIGURE 23 - PAINT CLEANING IN REINFORCED CARBON-FIBER PANELS. PANEL IIB

HYDRONAUTICS, INCORPORATED

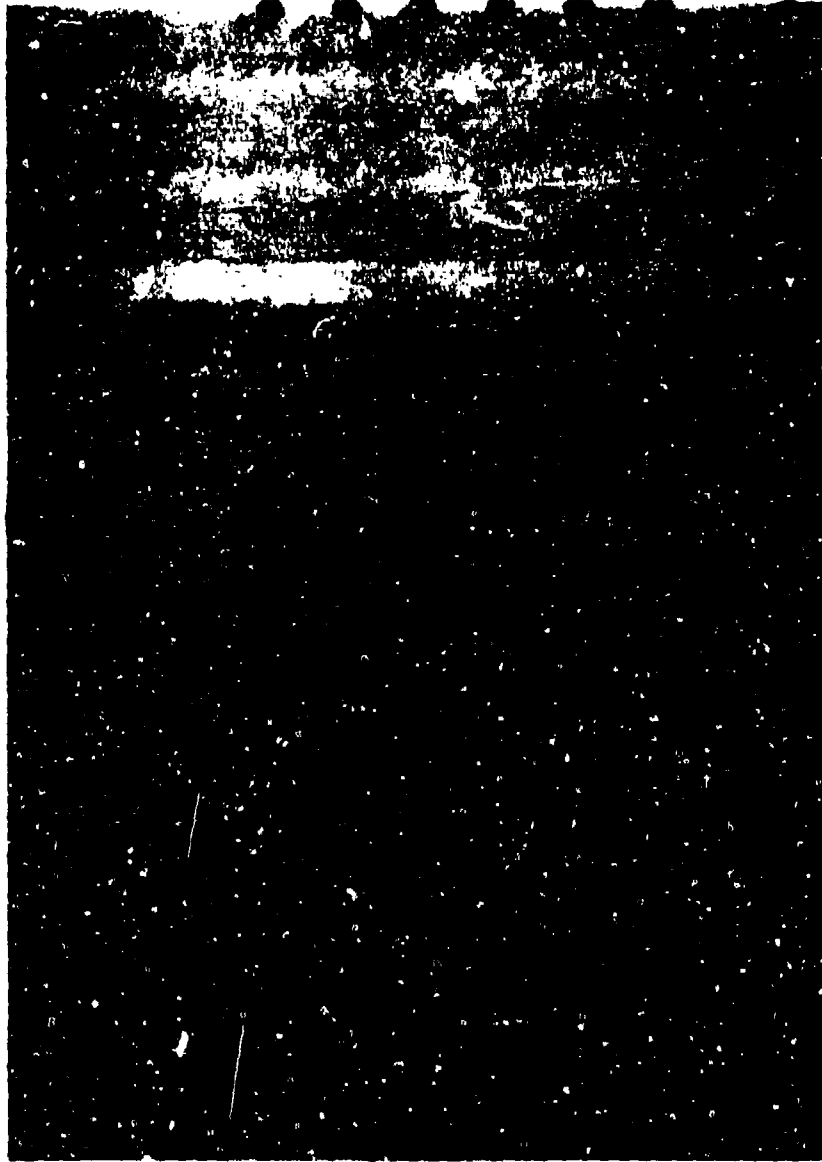


FIGURE 29 - PAINT REMOVAL PATHS ON ALUMINUM PANEL AT
SEVERAL STAND OFFS FOR THE SAME JET SPEED
AND TRANSLATION ($v_t = 1 \text{ in./s}$), LW : LEACH &

WALKER, $\Delta p = 5080 \text{ psi}$, PF : PULSER-FED,
 $\Delta p = 5400 \text{ psi}$.

HYDRONAUTICS, INCORPORATED

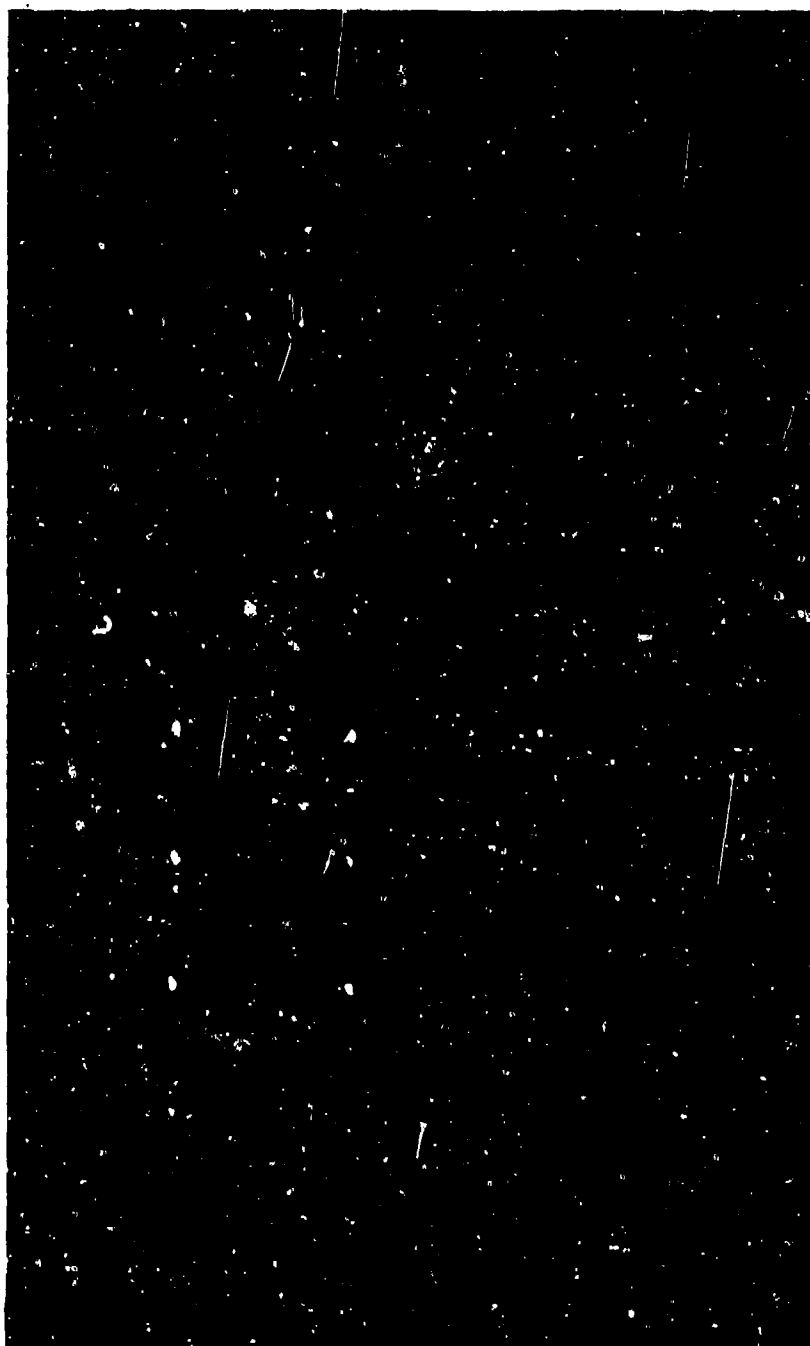


FIGURE 30 - PAINT REMOVAL PATHS AT A VARIABLE STAND
OFF DISTANCE, 11 INCHES $< X < 23$ INCHES,
1D : LEACH & WALKER, $\Delta p \approx 5080$ psi, 6B : PULSER-
FED, $\Delta p \approx 5400$ psi, $v \approx 1$ in./s

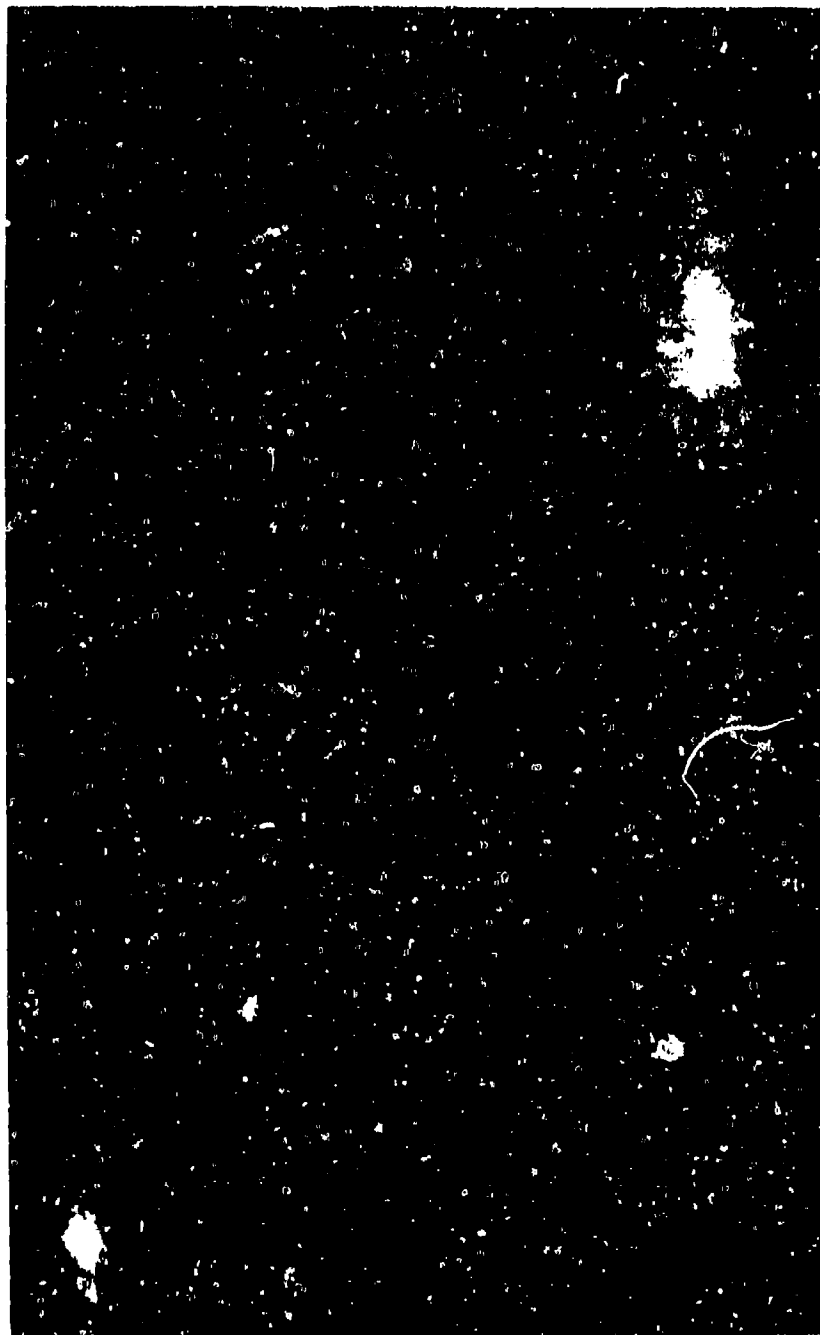


FIGURE 31 - PAINT REMOVAL PATHS AT THE OPTIMUM STAND
OFF DISTANCE: X = 13.5 INCHES, 8B : PULSER-FED
 $\Delta p = 5000$ psi, 3C : LEACH & WALKER, $\Delta p = 5080$ psi,
ALUMINUM PANEL V.

HYDRONAUTICS, INCORPORATED



FIGURE 32 - PAINT REMOVAL PATHS AT VARIOUS STAND OFF DISTANCES FOR THE SAME JET SPEED AND TRANSLATION VELOCITY. (COMPARE 3A AND 1A, 3B, 2A; 4A AND 5B) ALUMINUM PANEL V.

HYDRONAUTICS, INCORPORATED

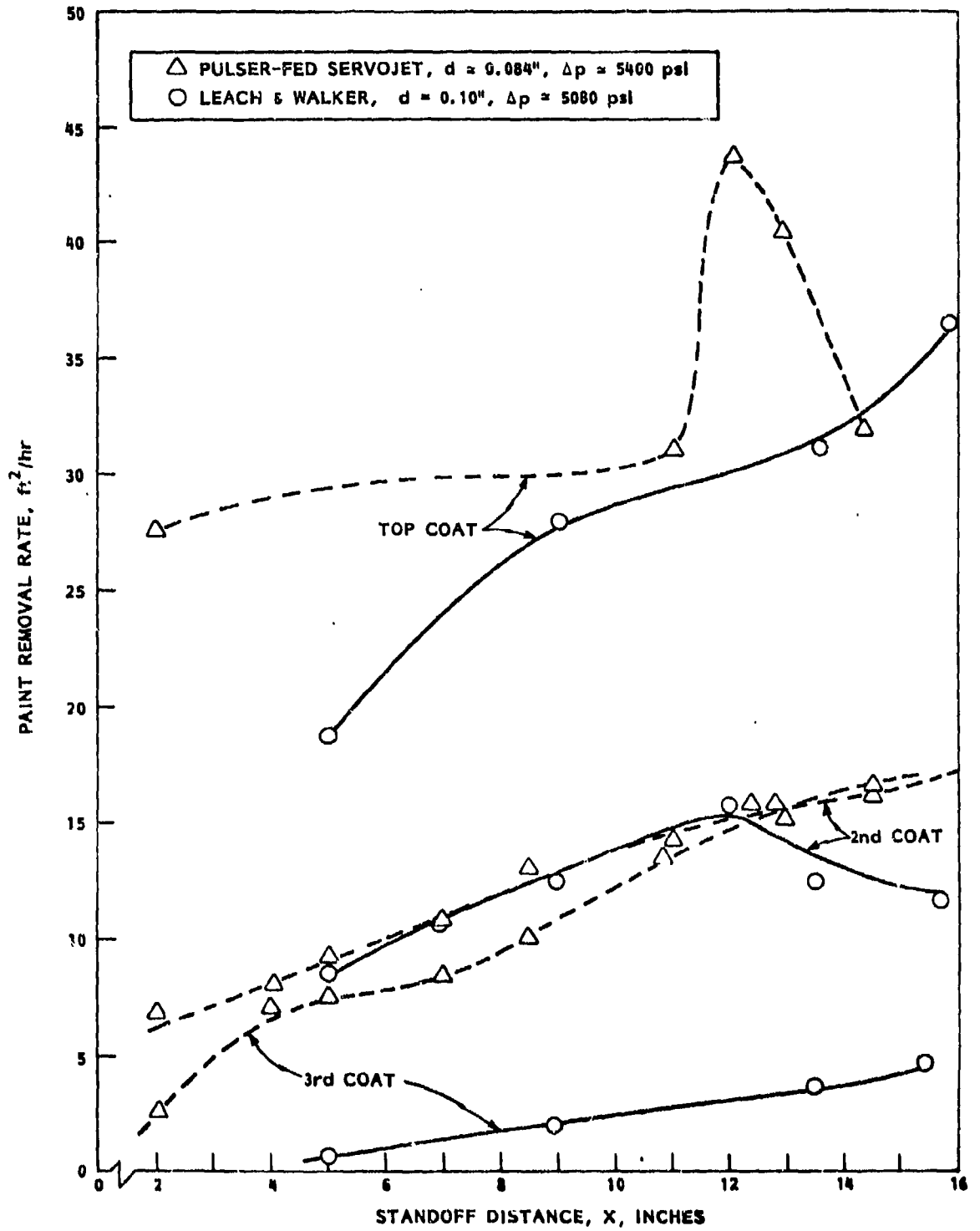
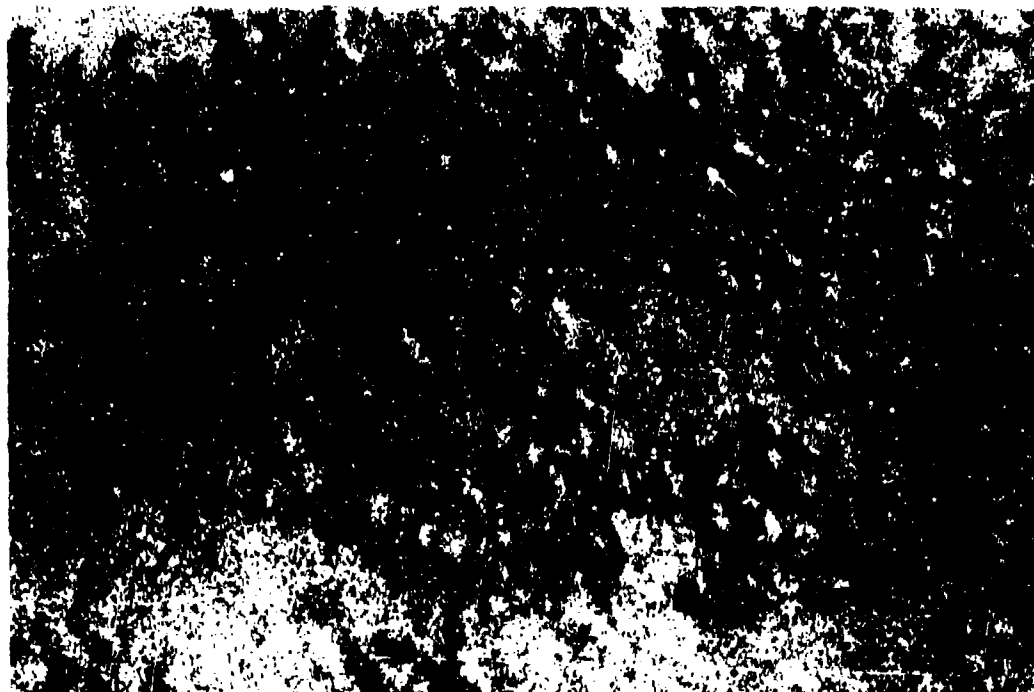
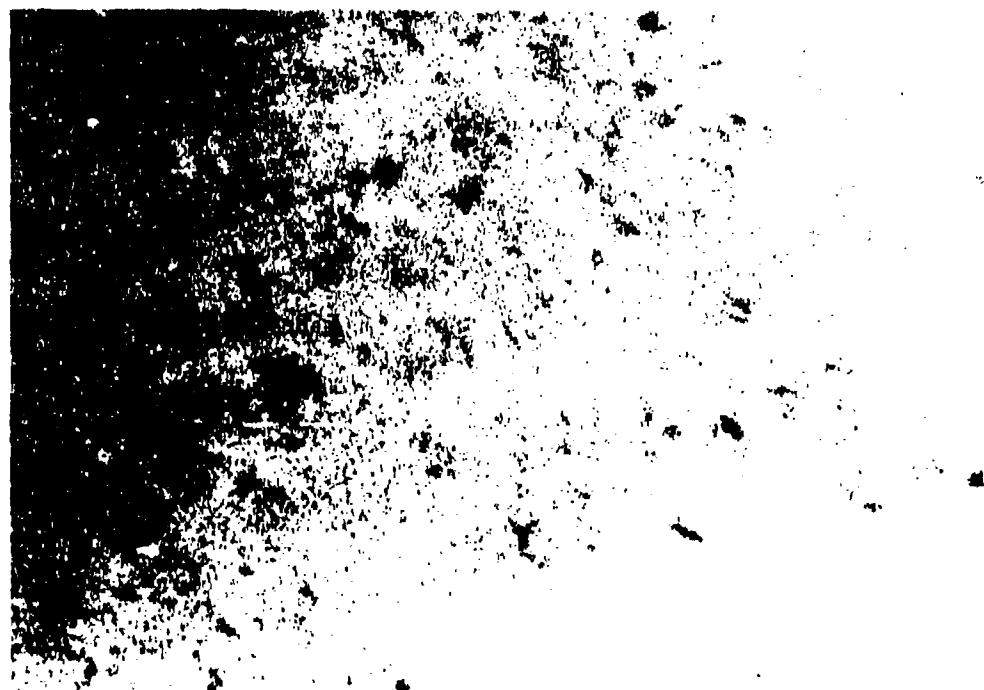


FIGURE 33 - REMOVAL RATE OF VARIOUS COATINGS ON ALUMINUM PANEL V. $v = 1$ inch/s



a. LEACH & WALKER



b. PULSER-FED SERVOJET

↑
0.5 mm
↓

FIGURE 34 - PHOTOMICROGRAPH OF THE PATHS FOR THE TWO JETS AT THEIR OPTIMUM PERFORMANCE

HYDRONAUTICS, INCORPORATED

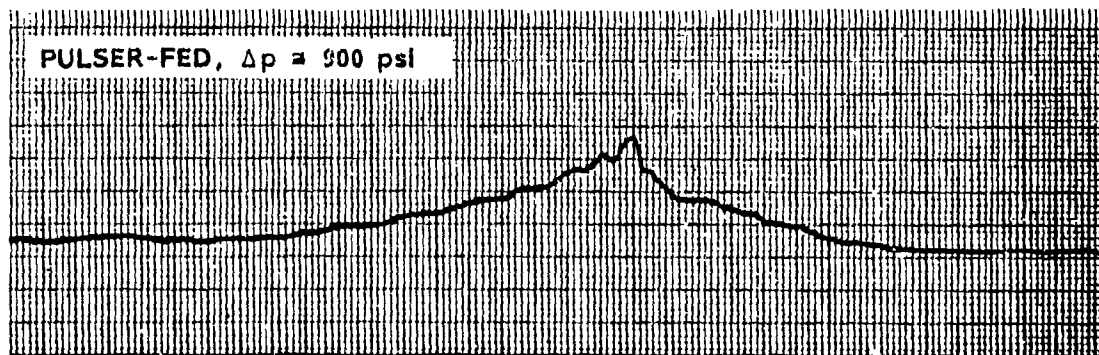
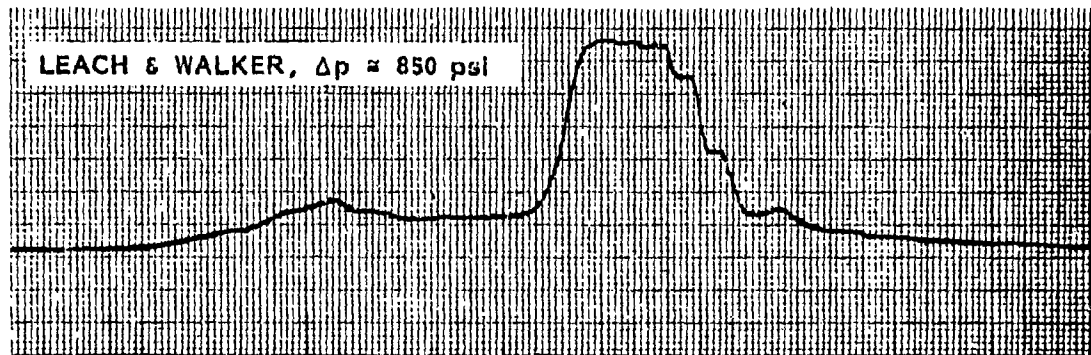
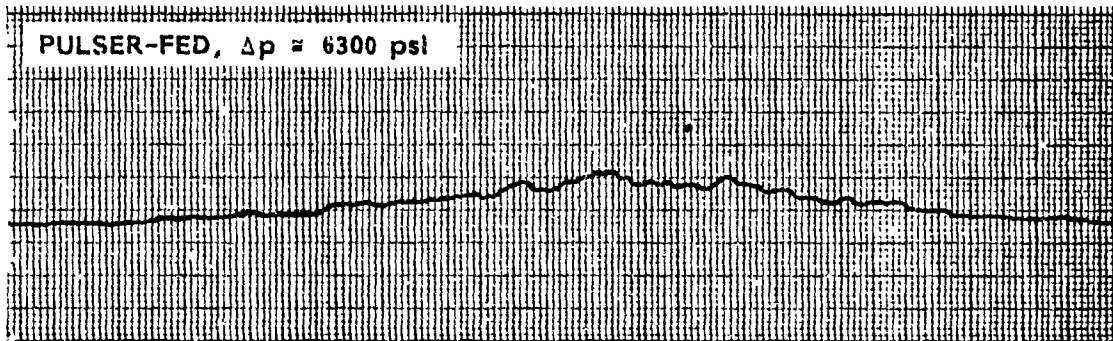
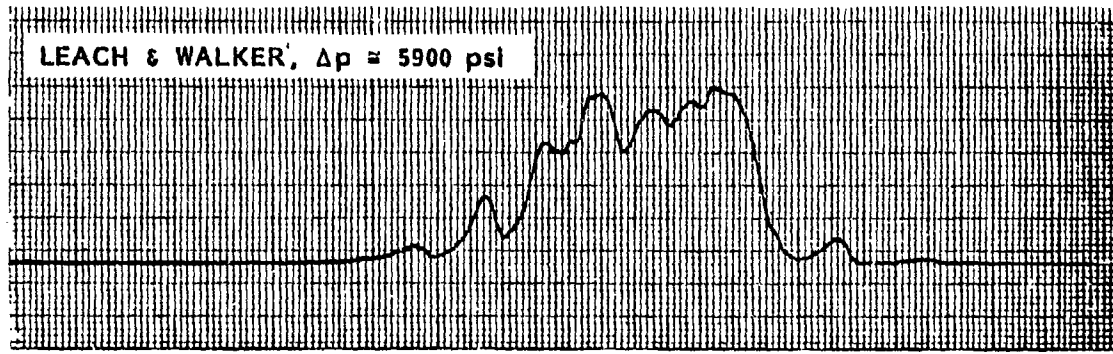


FIGURE 35 - PRESSURE PROFILE ACROSS THE JET, X = 13.5 INCHES